FREQUENCY SHIFTS INHERENT IN THE 6328 ANG. HELIUM-NEON LASER*

by

T. P. Sosnowski

W. B. Johnson

Technical Report No. A-57

November, 1967

*Supported in part by grants from the National Aeronautics and Space Administration, the Advanced Research Projects Agency and the Goodyear Aerospace Corporation.

ACKNOWLEDGEMENTS

The authors gratefully acknowledge the innumerable contributions of the staff members of Case Western Reserve University who assisted in this work. The efforts of Messrs. Edward Parillo and Imre Szilagyi, the glass blowers, and Mrs. Kathleen Smyth who helped prepare the manuscript are particularly appreciated.

This work was partially supported by grants from the National Aeronautics and Space Administration, The Advanced Research Projects Agency and the Goodyear Aerospace Corporation.

ABSTRACT

The effects of various discharge tube parameters on the center frequency of the Doppler-broadened ($3s_2$ - $2p_4$) 6328 Ang. lasing transition in Ne^{20} and Ne^{22} have been measured. Frequency shifts from 17½ to 23 MHz./torr were measured in the discharges depending on the combination of helium and neon isotopes used. The shift of the peak frequency with discharge tube current was immeasurable (< 1 MHz./10 ma.). In addition, it has been found that the peak frequency is dependent on the relative position of the tube axis with respect to the cavity axis, the variation for small bore tubes being of the order of 20 MHz./0.1 mm. Finally, an analysis is made of the possible causes for the pressure-frequency shifts, the result being that they may be attributed to collisions between the excited neon atoms ($3s_2$ level) and ground state helium atoms.

TABLE OF CONTENTS

APPENDICES

LIST OF FIGURES

LIST OF TABLES

I. INTRODUCTION

As is well known, the laser is a device which generates optical frequency radiation with properties very similar to that generated by lower frequency microwave oscillators. That is, the radiation is generally single frequency and, more importantly, coherent. It is found, however, that although the bandwidth of the laser radiation is very narrow (an experimentally measured value of 20 Hz. has been reported [1]), the frequency range over which the laser can operate is generally quite wide. In the helium-neon laser for example, it is determined by the Doppler broadening of the atomic transition responsible for the laser action and is of the order of 1.5×10^9 Hz. for the 6328 Ang. line. If some way can be found to control and easily reproduce the operational frequency of the laser, the device will find wide application in the fields of communications, metrology and high resolution spectroscopy.

Several laser frequency control schemes have been devised which utilize as a reference the center of the atomic resonance curve of the lasing transition. It is well known, moreover, that various discharge tube parameters such as gas pressure and current may alter the frequency of the peak of the gain curve [2,3]; thus, the reproducibility and stability of the frequency of this type of controlled laser ultimately depends on the discharge tube parameters which may affect the gain curve. This paper, then, is a report on an experimental study of the effects of these various discharge tube

parameters on the peak of the 6328 Ang. lasing transition in neon.

II. THE STABILITY OF THE GAS LASER

2.1 General characteristics

Before describing the details of this investigation, it is perhaps appropriate to review briefly a few of the more important frequency characteristics of lasers which pertain to this discussion. The operational frequency of a laser is determined by the frequency of the two closely coupled oscillators which make up the device:(1) the Fabry-Perot etalon, a multimode resonant cavity supplying feedback and (2) the system of atomic oscillators supplying the gain necessary for laser action.

The Fabry-Perot etalon is generally composed of a pair of mirrors, the surfaces being either plane or spherical and coated with multilayer dielectric films for ultra high reflectance (>99%). Consider a cavity composed of a spherical mirror (with radius of curvature R) and a flat mirror separated by a distance L < R as shown in Fig. 2.1.

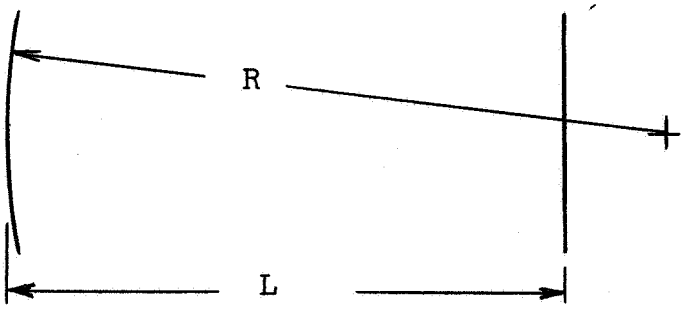

Fig. 2.1. Plano-concave etalon

The resonance condition of this cavity for radiation of wavelength λ is given by [4]

$$\frac{2L}{\lambda} = q + \frac{1}{2\pi} \left(1 + r + s \right) \cos^{-1} \left(1 - \frac{2L}{R} \right) \qquad (2.1)$$

q being the longitudinal, and r and s the transverse mode numbers. Normally the laser is made to operate in the lowest order transverse mode so that $r = s = 0$. The resulting second term on the right of equation 2.1 has a maximum value of one whereas $q = 2L/\lambda \approx 10^6$; thus the former may be neglected. The values of λ satisfying the cavity resonance condition are then

$$\lambda = 2L/q;$$

in terms of the frequency ν_c this becomes

$$\nu_c = qc/2L. \qquad (2.2)$$

It must be remembered that L here is the value of the optical path length in the cavity; it is related to the geometrical path length L' by $L' = L/n$ where n is the index of refraction of the medium between the mirrors.

The frequency difference $\Delta\nu_q$ separating two adjacent modes is found directly from equation 2.2 and is given by

$$\Delta\nu_q = c/2L$$

For a typical one meter mirror separation, $\Delta\nu_q$ is about 150 MHz. The introduction of an active medium in the cavity to provide gain

for the laser introduces various mode pulling effects and changes the value of $\Delta\nu_q$ somewhat, but these are second order and may be neglected in the present analysis.

Consider now the system of atomic oscillators; the full width at half maximum intensity of the resonance curve is determined by Doppler broadening and is given by

$$\Delta\nu_D = 2\nu_o \left[\frac{2kT}{Mc^2} \ell n2\right]^{\frac{1}{2}}$$

where ν_o is the frequency of the atomic line center, M is the mass of the atom involved, k is Boltzman's constant, T is the temperature, and c is the velocity of light. For the 6328 Ang. line this is about 1.5×10^9 Hz. If it is assumed that the gain of the laser is greater than the loss over this band of frequencies (an easily obtainable experimental situation) a laser with a one meter cavity will oscillate in at least ten distinct axial modes. This is depicted in Fig. 2.2.

Generally it is desired to operate the laser in a single mode. This may be accomplished by special mirror configurations [5] or by decreasing the length of the laser cavity until $\Delta\nu_q$ of equation 2.3 is greater than the width of the atomic resonance over which the gain exceeds the loss as illustrated in Fig. 2.3. The length of such a short cavity is typically of the order of 10 to

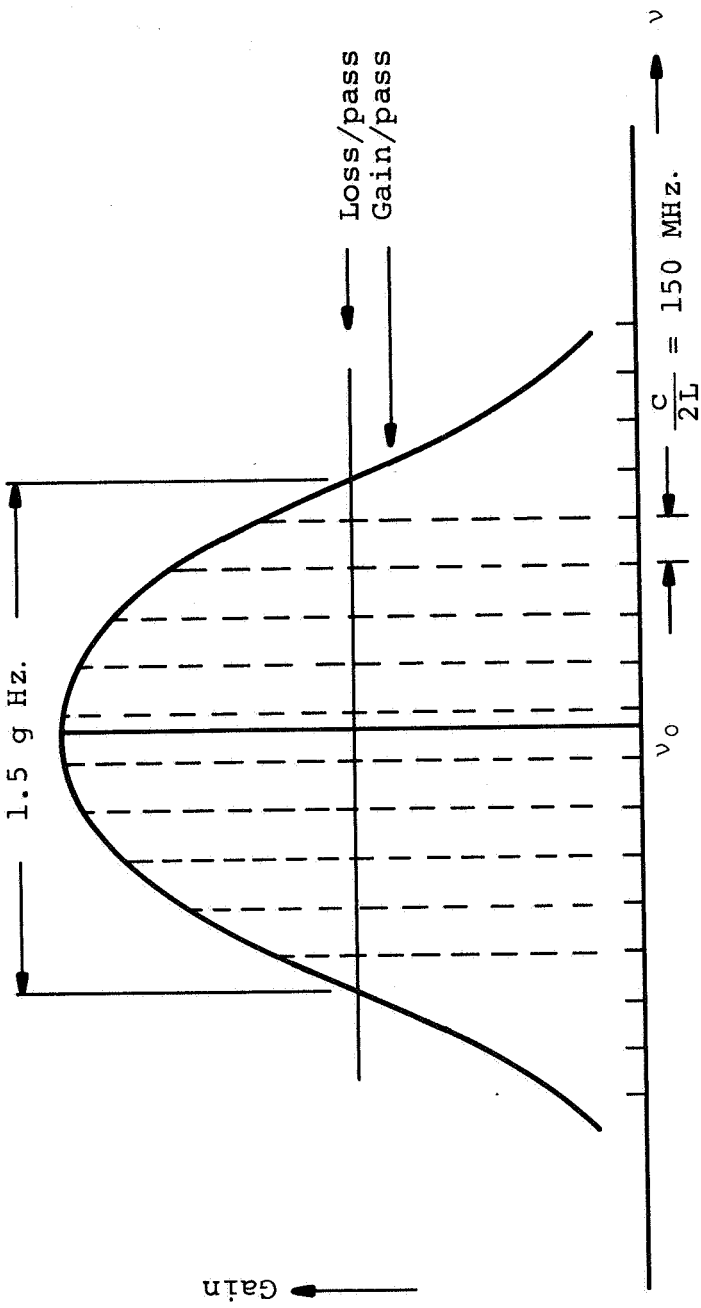

Fig. 2.2 Gain profile and longitudinal cavity resonances for a one meter cavity. The dashed lines represent lasing modes.

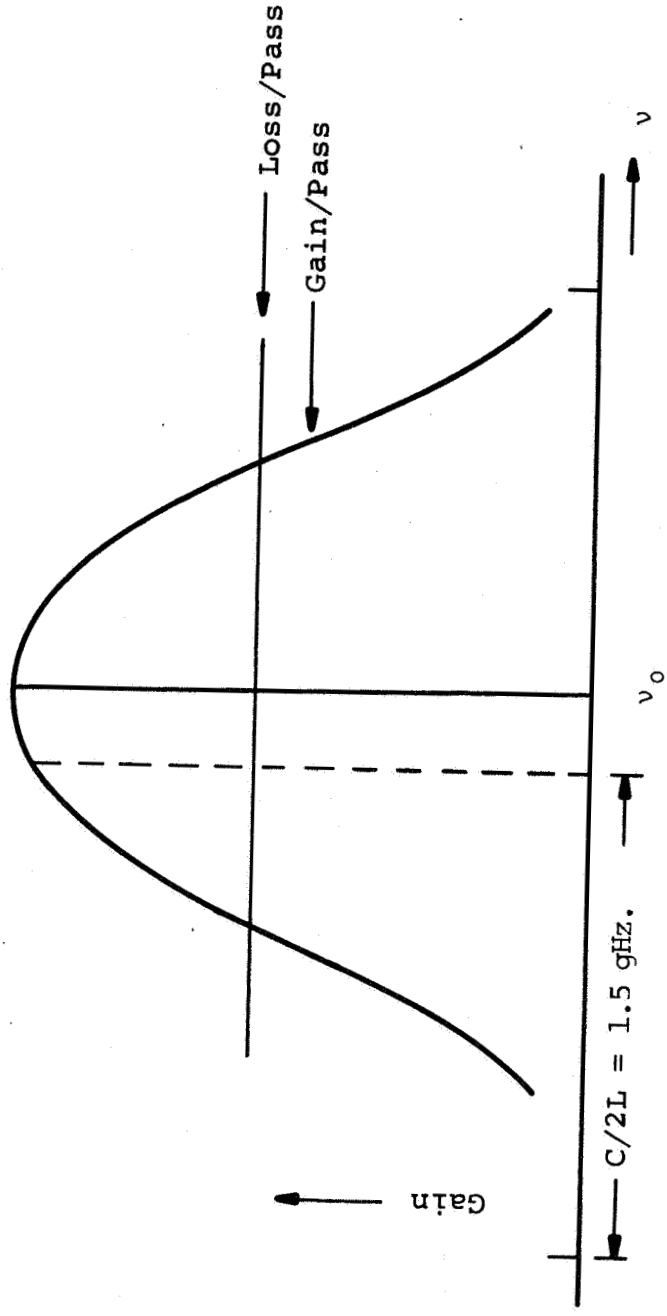

Fig. 2.3 Gain profile and longitudinal cavity resonances for a 10 cm. laser cavity

15 cm. Although this type of laser does operate in only one mode, the actual value of the frequency will vary with the mirror separation in accordance with equation 2.2. The range of frequencies over which the output will vary is found to be roughly equivalent to the Doppler width or about 1.5×10^9 Hz.

Various methods can now be used to stabilize the free running laser so that the frequency is limited to essentially a single value. Generally they consist of three classes of systems. Two of them, one based on two beam interferometry [6,7,8] and another based on high Q resonant optical cavities [9], essentially depend on maintaining a fixed optical path length in some medium and using it as a reference. The third class uses the center of the atomic resonance as a reference [10 - 14]. The assets and liabilities of the first two types are well documented in the cited literature. Concerning the third class, the systems have been rigorously treated and expressions have been derived for the stabilities to be expected [11] - all based on a stationary atomic resonance curve. In order to obtain a true measure of the stability of this type frequency controlled laser, the variability of the gain curve peak frequency must be considered.

2.2 Stability Criteria

The concept of stability has been encountered above; it is in order at this point to specify what is meant by it and to indicate what the fundamental limitations are on the stability of the gas

laser. Frequency stability may be defined by

$$S_\nu(\tau) = \nu / \Delta\nu(\tau) \qquad (2.4)$$

where ν is the average frequency of operation of the laser and $\Delta\nu(\tau)$ is the fluctuation in frequency over some period of time τ. Two types of stability are commonly encountered in the description of laser operation: the short and the long term stability, the latter being applicable if the time is greater than the limit of the time resolution of the detection system used [15].

The ultimate limit to the short term frequency stability is determined by spontaneous emission into the oscillating mode of the laser which produces irreducible fluctuations in the laser frequency; it is given by [16, 17]

$$\Delta\nu = 2\pi h\nu \ \Delta\nu_c^2/P$$

where P is the output power of the laser, h is Planck's constant, and $\Delta\nu_c$ is the full width at half maximum of the cavity resonance. Typically $\Delta\nu$ is about 10^{-2} Hz. for output powers of about one milliwatt. The long term frequency stability of a free running laser is primarily determined by the stability of the Fabry-Perot resonator. For perturbations affecting the cavity length, the frequency stability is found from equations 2.2 and 2.4 to be

$$S_\nu = L/\Delta L.$$

The mirrors are separated by spacer rods whose length will vary as a result of thermal excitation of the lowest frequency stretching modes in the material. This produces a fractional change in length given by [1]

$$\Delta L/L = (2kT/YV)^{\frac{1}{2}}$$

where V is the spacer rod volume and Y their Young's modulus. Considering a 15 cm. long cavity with spacer rods of steel of total cross sectional area 20 cm^2, the frequency fluctuation is about 5 Hz. producing a resultant frequency stability of about 10^{14}. This probably represents the fundamental limitation on the stability of the gas laser. Comparing this with what has been achieved in practice, lasers stabilized on the center of the gain curve have achieved stabilities approaching 10^{10} for periods of several hours [12]

2.3 Causes of instability in the gas laser

In treating the causes of instabilities in a gas laser, we must carefully distinguish between those to which the free running and the frequency stabilized laser are principally subject. The stabilized laser is, of course, affected by the same type of perturbations as the free running device; in fact, it is the purpose of the stabilizer unit to compensate for these and allow the laser to generate a discrete frequency. In addition, since the stabilizer units considered here utilize the peak of the atomic gain curve as a reference, any variation in the frequency of the peak manifests

itself as an instability in the frequency controlled laser signal. The treatment of the peak frequency variation will be deferred to a later chapter.

The remaining causes of instability are primarily a result of modifications in the cavity resonance brought about by variations of the optical path length between the two mirrors. They may be conveniently divided into the following categories:

A. Effects internal to the discharge tube
   1) Fluctuations in electronic refractivity.
   2) Fluctuations in atomic refractivity associated with the laser transition.

B. Effects external to the discharge tube
   1) Motion of the mirrors.
   2) Changes in the refractive index of the air (for external mirror lasers).

Of those effects internal to the discharge tube, variations in the electron density will have a negligible effect on the index of refraction within the tube [9]. Frequency variations due to fluctuations in refractive index of the inverted populations are not usually observed unless the discharge is noisy; at line center, where the susceptibility vanishes, they have a negligible effect on the cavity resonance [13].

The principal factors affecting the free running laser stability, then, are found outside of the tube. Generally, acoustic

and building vibrations coupled into the supporting structures of the mirrors are responsible for their vibration. The magnitude of the problem is evident from the fact that a 3 Ang. change in mirror spacing of a 15 cm. long 6328 Ang. laser produces a frequency shift of 1 MHz. The effects of vibration are usually mitigated by careful selection of the laser environment, i.e., special platforms in isolated rooms.

Changes in temperature, pressure and humidity are responsible for most of the long term drift in the cavity resonance; the temperature causes material expansion resulting in a change in mirror separation, all three change the refractive index of the air. The effect of a change in temperature of the spacers between the mirrors is given by

$$\Delta\nu/\nu = \alpha\Delta T$$

where α is the coefficient of expansion of the spacer material. For a spacer of quartz, $\Delta\nu \approx 250$ MHz./^{o}C; for one of iron $\Delta\nu \approx 5000$ MHz./^{o}C. The effect of refractive index changes on the frequency is given by [15] to be:

$$\Delta\nu/\nu = \beta_T \Delta T + \beta_p \Delta p + \beta_h \Delta h$$

where the β's are the logarithmic change of the index of refraction with respect to temperature, pressure and humidity. Specifically they can be evaluated to be:

$$\beta_T = \frac{1}{n}\frac{dn}{dT} = -\ 9.3 \times 10^{-7}\ /^{\circ}C$$

$$\beta_p = \frac{1}{n}\frac{dn}{dp} = \quad 3.6 \times 10^{-7}\ /\text{torr}$$

$$\beta_h = \frac{1}{n}\frac{dn}{dh} = -\ 5.7 \times 10^{-8}\ /\text{torr}$$

for $T = 20^{\circ}C$, $p = 760$ torr, $h = 8.5$ torr water vapor pressure and $\lambda = 6328$ Ang.

We have seen from the above account that the laser frequency is primarily determined by the laser cavity mirror separation, or, more precisely, by the optical path length between the two mirrors. Various disturbances and their effect on the laser frequency have also been noted and these amply justify the need for a laser frequency control system. Such a system, using as a reference the peak frequency of the gain curve, does not uniquely determine the laser frequency, however, because the peak frequency itself is not unique but is subject to certain discharge tube parameters. It is the object of the present work, then, to determine under what circumstances and to what extent the peak frequency does shift. The following chapter is a detailed description of the apparatus used to conduct this investigation.

III. DESCRIPTION OF EXPERIMENTAL APPARATUS

3.1 Experimental Method

Basically the experiment reported herein consists of the solution of two problems: (1) Operation of the laser in a mode corresponding to the center frequency of the 6328 Ang. transition in neon and (2) measuring the shift in center frequency as various discharge tube parameters are changed.

As pointed out earlier, many schemes have been advanced for the operation of a laser at the center of the gain curve. The one used here is an adaptation of a version originally proposed by Rowley and Wilson [10]. Its operation can easily be described with the aid of Fig. 3.1 which shows the idealized laser intensity as a function of frequency. Perturbation of the cavity length will frequency modulate the laser giving rise to an amplitude modulation. Perturbation at a frequency ω around point a in the diagram amplitude modulates the laser beam intensity at ω with a phase relationship as shown (increasing the laser frequency increases the output power). Perturbation around point b again gives rise to the same frequency; now, however, the phase relationship between the two signals differs by π from that at point a (increasing the laser frequency decreases the output power). With perturbation around c, the fundamental

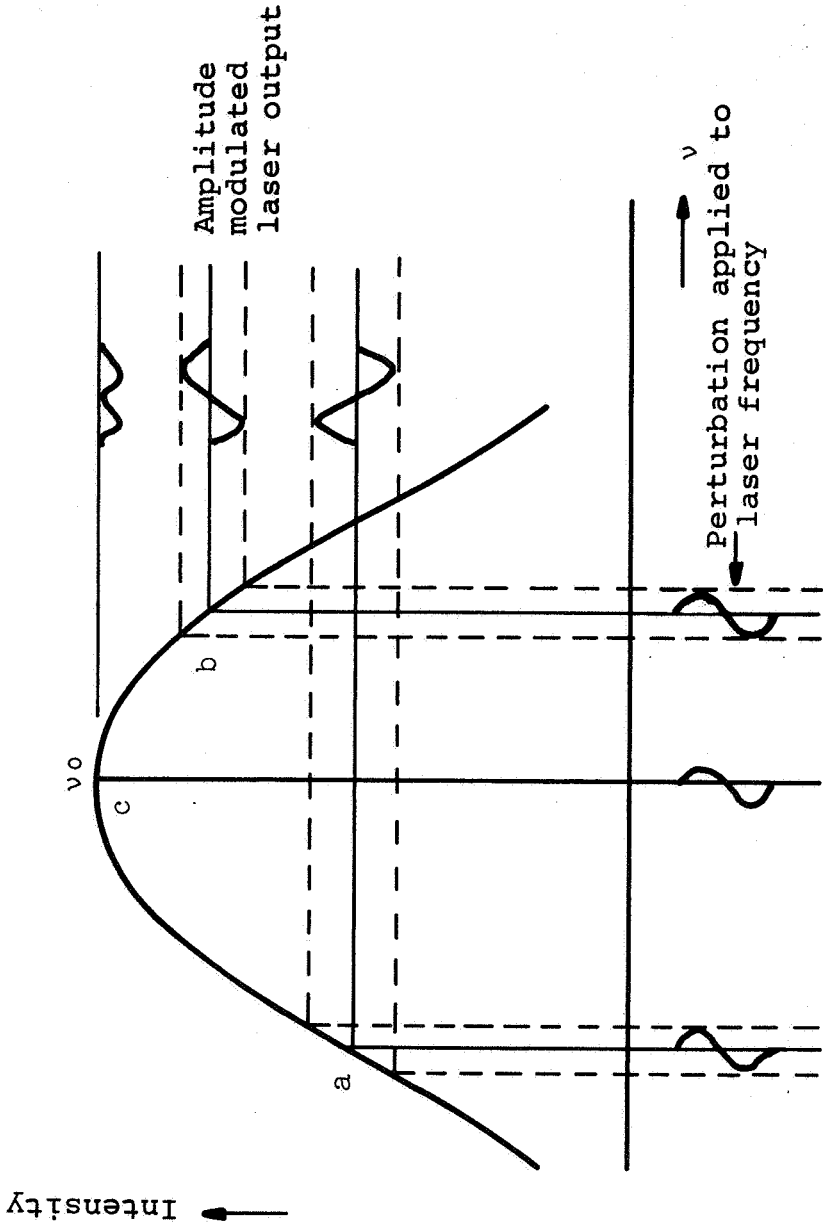

Fig. 3.1 Gain profile of a laser showing phase relationship between input and output perturbation

frequency vanishes from the beam and essentially only the second harmonic remains.* It is thus possible to determine where the laser is oscillating relative to the center of the atomic transition with the aid of a phase sensitive detector.

Actually, a power dip (the Lamb dip [19]) rather than a maximum is found as the laser is tuned through the peak frequency, and it is this minimum which is used as a reference. It arises because of saturation effects in the laser; the position is coincident with line center and the exact shape is related to the radiative lifetimes of the levels and details of the collision mechanisms involved [20]. It has the general properties of being narrower at lower pressures and deeper at higher output powers. The Lamb dip is clearly illustrated in the oscillograph of Fig. 3.2 which presents, in the lower trace, the amplitude vs. frequency characteristic of the laser. The small oscillation on the right peak is a result of ringing in the piezo-electric crystal used to drive the mirror (see below) and is not characteristic of the gain curve.

Since no frequency standard exists in the visible portion of the electromagnetic spectrum, it is impossible to measure the absolute laser frequency. The most information that can be obtained is the relative frequency difference between the laser and some

---

*A mathematical derivation of this may be found in Appendix A.

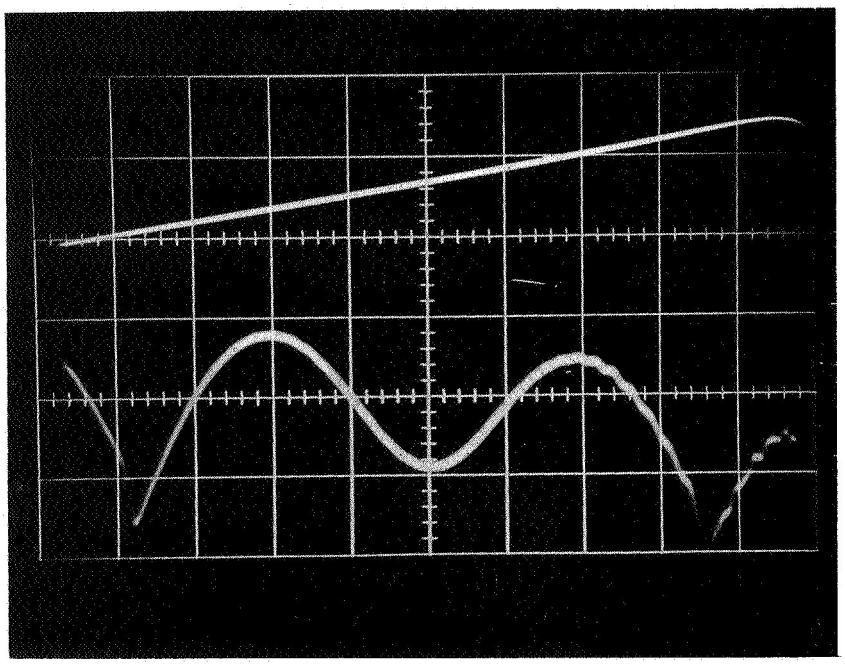

Fig. 3.2. Lower trace is the amplitude versus frequency characteristic for the He^3-Ne^{20} laser showing the power dip at the peak of the gain curve. The cavity length was 37 cm. The upper trace represents the voltage applied to the piezo-electric ceramic; amplitude: 100 v./cm.

arbitrary reference. In this experiment a laser similarly stabilized on the bottom of the Lamb dip was used as a reference, the difference in frequency being determined by optical heterodyne techniques.

A schematic diagram of the experiment is shown in Fig. 3.3. The amplitude modulated laser beam is detected by the frequency control phototube and sent to the frequency control unit; here an error signal is generated allowing the laser frequency to be positioned at the atomic line center. At the other end of the cavity the two laser beams are superimposed by means of the mirror and beam splitter and passed on to the phototube where the heterodyne signal is detected. As various parameters of the signal laser are changed, both lasers are centered on their respective gain curves and their difference frequency observed on the spectrum analyzer.

3.2 Laser Peak Frequency Sensing Device

A block diagram of the system used to sense the peak* in the laser gain curve is shown in Fig. 3.4. A 5 kHz. audio frequency is used to perturb the laser frequency resulting in an amplitude modulated output from the laser. The signal is detected by a photomultiplier tube whose output is fed into a 5 kHz. amplifier with 60 db. voltage gain and a bandwidth of 500 Hz. This signal is then

*Henceforth, the frequency at the bottom of the Lamb dip will be referred to as the peak frequency.

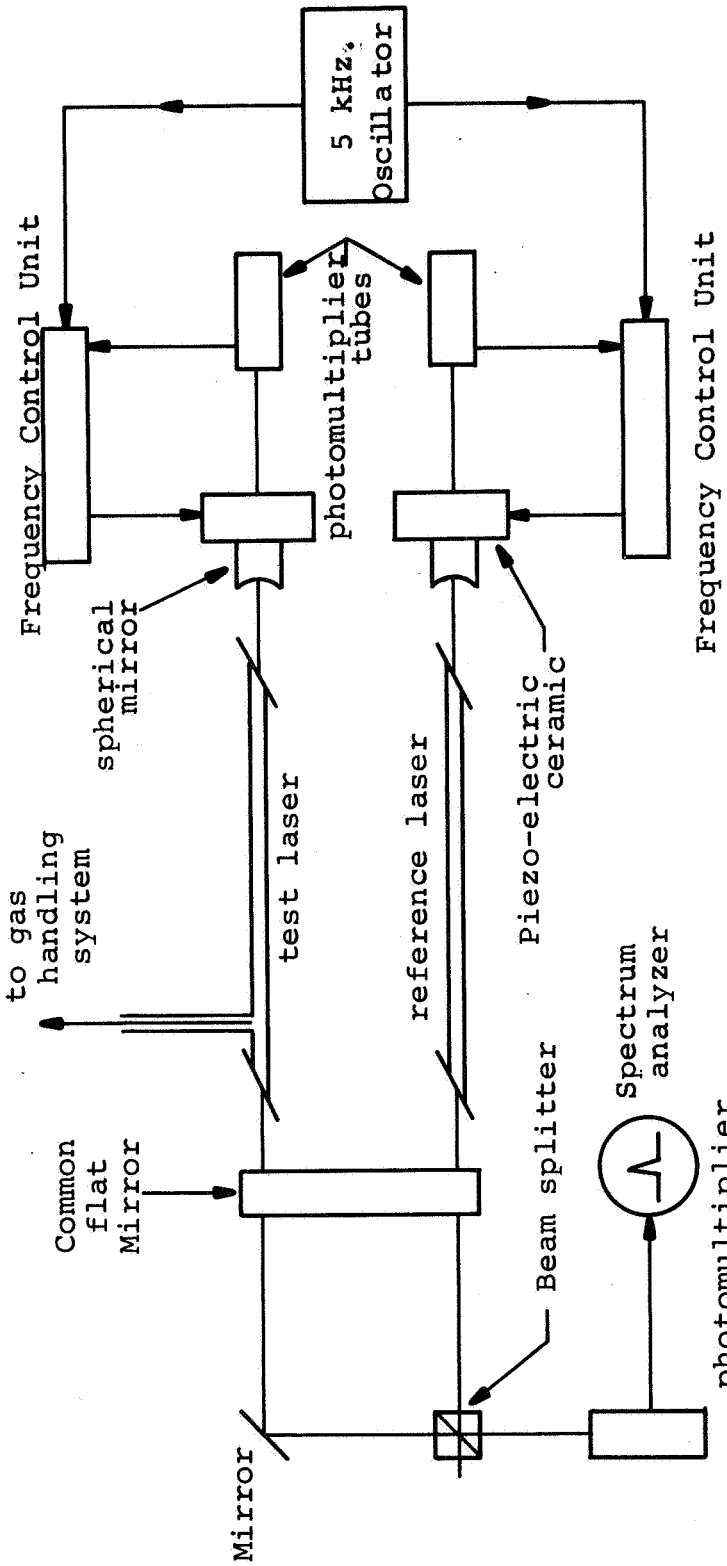

Fig. 3.3 Schematic diagram of apparatus used to measure frequency shifts with pressure in the He-Ne laser

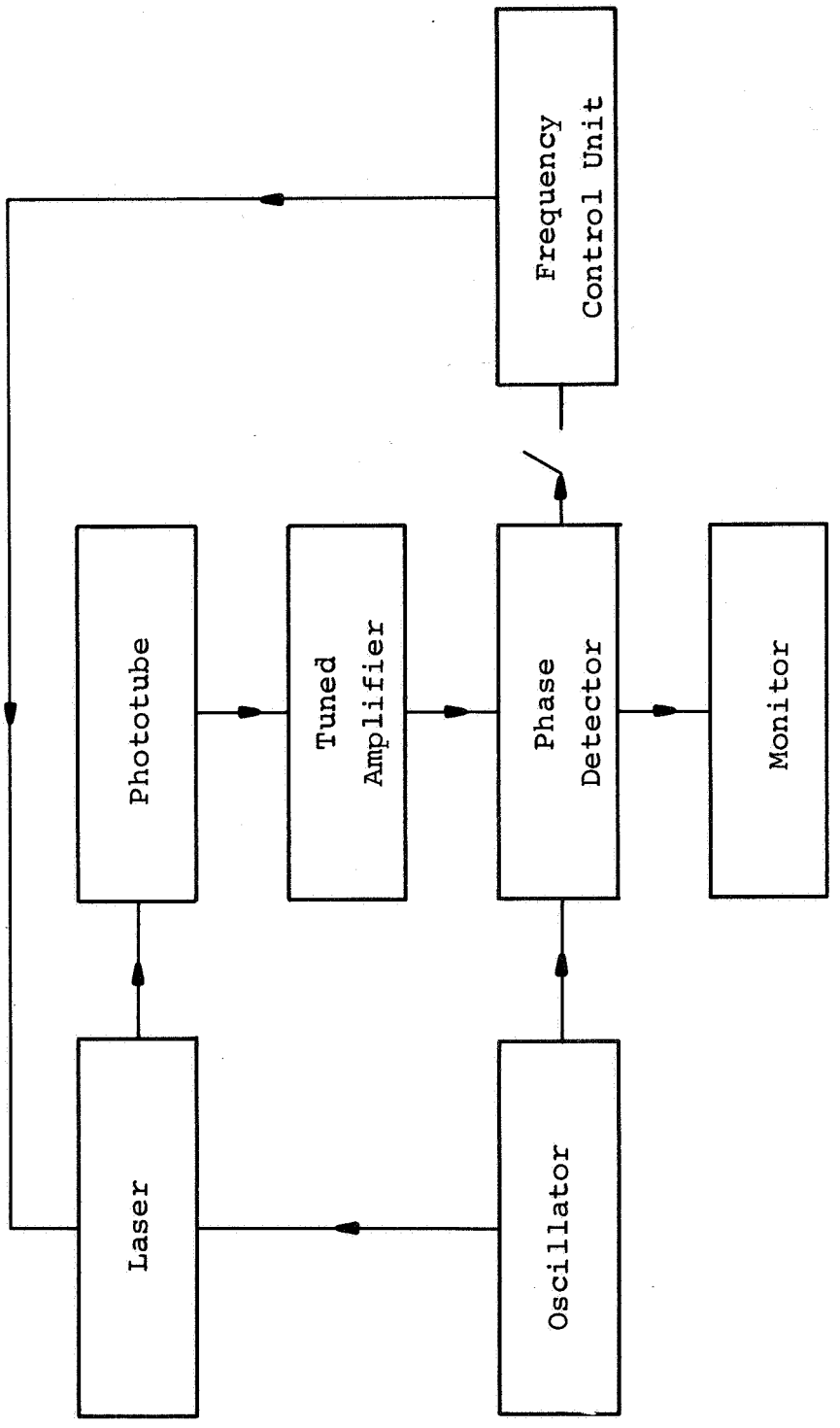

Fig. 3.4 Block diagram of laser peak frequency control system

combined with the oscillator signal in a phase sensitive detector. The signal generated here is fed into a suitable readout device which then enables the operator to adjust the cavity length and position the laser frequency on line center. Alternatively, this can be done automatically by sending the error signal generated by the phase detector directly to the cavity length control.

A piezo-electric ceramic device* attached to one of the mirrors serves to physically control the laser frequency. A small sinusoidal voltage applied to the ceramic perturbs the cavity length while a d.c. bias voltage is used to control the absolute length of the cavity. The voltage required to lengthen the crystal increases with frequency (neglecting resonances) and is about 500 volts/micron at 5 kHz.

A useful error signal could be extracted from the laser at perturbation frequencies well beyond 50 kHz. despite the large size of the quartz mirror (3/8 inch in diameter x 3/8 in. thick) attached to the ceramic. Ultimately, 5 kHz. was selected for use because of the lower voltages needed to drive the ceramic at this frequency. Also, in some bands of frequencies above 10 kHz., the laser frequency was found to anomalously jump across certain regions

---

*Obtained from the Clevite Corporation, Cleveland, Ohio. It is ½ inch thick and ½ inch in diameter with a 1/8 inch hole through the center to permit passage of the laser beam. It is constructed of a series of 10 disks of PZT-5A ceramic separated by metal electrodes; this construction allows the use of relatively low voltages to obtain the necessary mirror movement.

of the gain curve. Under these conditions, the perturbation of the laser amplitude could no longer be simply related to the frequency perturbation as expected by the description of section 3.1.

The amplitude of the voltage applied to the crystal and hence the amplitude of the intensity perturbation of the laser was dictated by the need to overcome the noise generated in the laser discharge tube. This noise is strongly dependent on the discharge tube current, gas pressure and composition. That this, and not the noise in the phototube, is the principal source of noise in the system may be shown by a comparison of the calculated shot noise current with the noise current actually measured. The noise current generated in the phototube is given by [21]

$$\overline{i_n^2} = 2\eta\, e^2\, P\, \Delta f/h\nu$$

where η is the quantum efficiency, e the electron charge, P the laser power, Δf the detection frequency bandpass, and $h\nu$ the quantum energy. Assuming a quantum efficiency of .01, a laser power of one milliwatt and a band pass of 500 Hz.,

$$\overline{i^2} \approx 10^{-21}\ \text{amp}^2.$$

This is to be compared with the value of the measured noise current:

$$\overline{i_n^2} \approx 10^{-12}\ \text{amp}^2.$$

The possibility exists that the noise is induced by environmental disturbances such as acoustic and building vibrations.

This hypothesis was tested by monitoring the outputs of two closely coupled lasers which would be identically affected by vibrations (see section 3.5 below). Fig 3.5 shows two representative oscillographs (taken at different sweep speeds) comparing the output fluctuations of the two beams; clearly some correlation would exist between the two traces on each oscillogram should the disturbance be common to both lasers. No such correlation appears to exist.

The minimum perturbation amplitude applied to the laser which would yield an adequate and unambiguous output from the phase sensitive detector corresponds to about a 1 MHz. modulation of the laser frequency. For a 15 cm. cavity, this is equivalent to a change in length of 3 Ang. or a peak to peak voltage on the piezoelectric ceramic of 150 mv. Obviously, the amplitude of the intensity modulation depends on the frequency position beneath the gain curve.

3.3 Vacuum and gas handling system

The vacuum and gas handling system is composed entirely of glass. It utilizes a conventional forepump coupled with a liquid nitrogen cold trap and a Varian Associates 8 l./sec. Vac-Ion pump. This combination permitted the evacuation of the system in excess of 10^{-7} torr. A consolidated Vacuum System McLeod gauge was used to measure all gas pressures with measurements reproducible to within $\pm$ .02 torr. A Pirani gauge was also incorporated in the system to allow immediate, but approximate, pressure measurements.

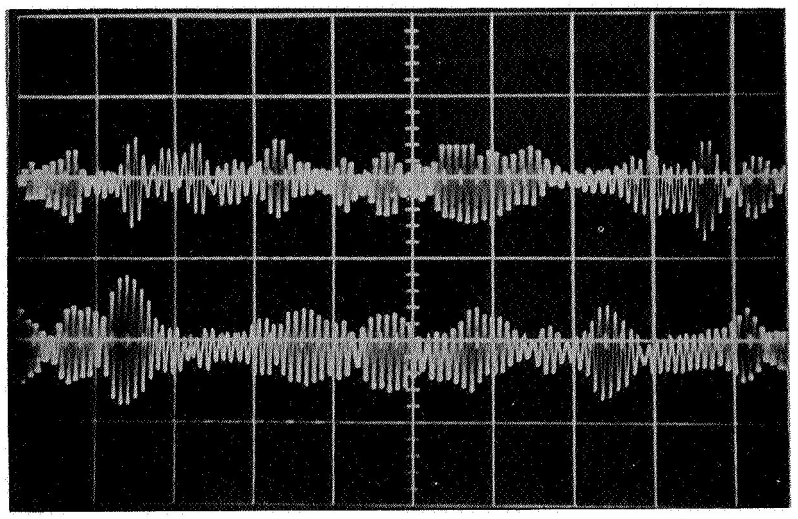

Horizontal sweep: 2 msec./cm.

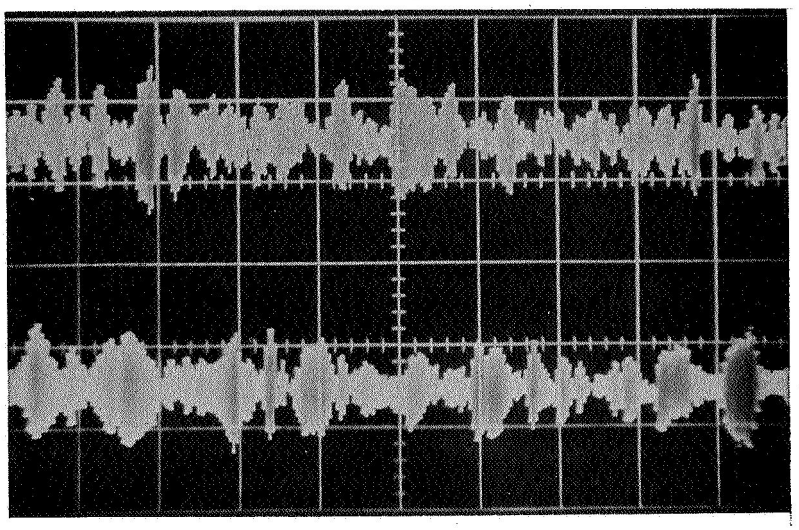

Horizontal sweep: 5 msec./cm.

Fig. 3.5. Oscillographs comparing 5 kHz. noise generated by two closely coupled lasers. Upper trace represents laser #1; lower trace, laser #2.

To produce the necessary pressure changes the laser tube was filled to its maximum operating pressure* and then exhausted in discrete steps, a frequency measurement being taken at each step. To decrease the pressure, a glass stopcock between the McLeod gauge and the vacuum system was rotated quickly in its seat allowing a small volume of gas to escape from the McLeod gauge; a valve between the laser and the gauge was then opened allowing the pressure to equalize between the two. This roundabout method was followed as a precautionary measure to help prevent a mixture change due to a difference in diffusion rates between the two constituent gases.

3.4 Environment

The need for adequate isolation of the lasers from environmental disturbances has been previously demonstrated. Isolation of the laser from the effects of building vibrations was achieved with the construction of a special structure in a ground floor laboratory. It consisted of three alternating layers of plywood and "rubberized hair"† on top of which was placed an iron surface plate estimated to weigh 3000 pounds. Six inflated

---

*In a 1 mm. bore tube and a current of 3 ma. the discharge becomes excessively noisy at pressures between 3½ and 5 torr depending on the He-Ne partial pressure ratio; the higher the helium partial pressure, the higher the pressure could be raised before the onset of noise. The pressure ratios used extended from 5:1 to 11:1, He-Ne.

†Packing material available from Jenkins Paper and Box Co., Cleveland, Ohio.

automobile inner tubes were placed on top of this followed by a stack of approximately two feet of plywood sheeting. Atop this was placed another iron surface plate estimated to weigh 1000 pounds. The entire vacuum system, except for the fore pump, as well as the lasers was attached to the top of this table. The resonance frequency of the structure with damping neglected was calculated to be 5 Hz. The damping provided by the plywood at this frequency prevented the observation of any vertical resonance, however. Fig. 3.6 is a photograph of the arrangement. Further isolation was achieved by locating the supporting structure in a room apart from that occupied by the operator and necessary control and monitor equipment.

3.5 The lasers

The lasers are of standard design and were constructed in this laboratory. They utilize Brewster's angle windows to allow use of external mirrors. Excitation is provided by a hot cathode d.c. discharge. It was found necessary to excite the filaments by direct current as alternating current modulated the discharge and hence the laser output. The bore diameters varied from 1 to 3 mm. and the active discharge length from 10 to 35 cm. depending on the cavity length requirements. The discharge current was obtained from a regulated voltage source. In addition, each laser tube was surrounded by mu-metal to shield it from the effects of background magnetic fields.

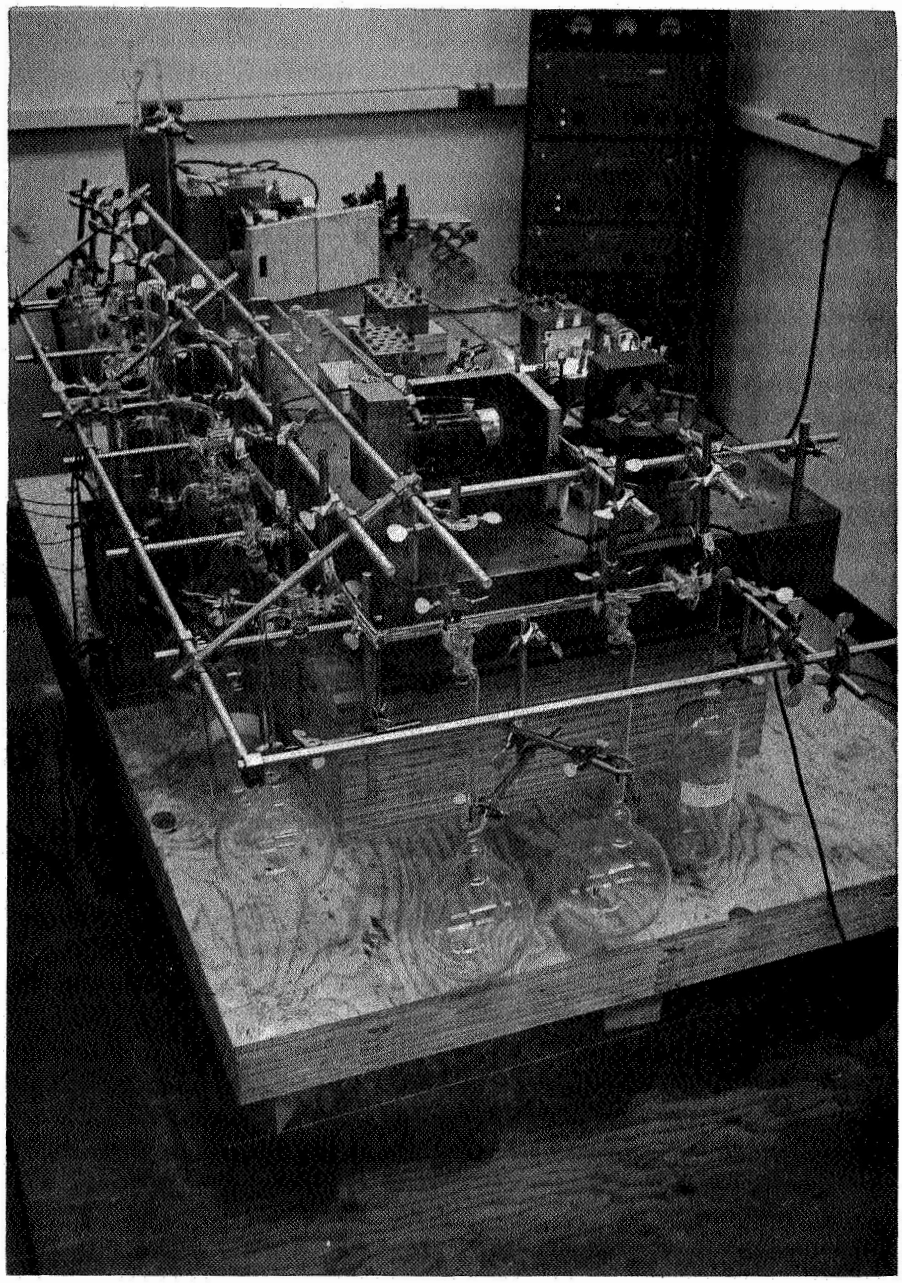

Fig. 3.6 Photograph of Laser Support System.

3.6 The dual cavity arrangement

As indicated in section 3.1, the frequency shift of the "test" laser is measured by optically heterodyning its output with that of a second laser (called the reference laser) to generate a difference frequency. The cavity arrangement employed is shown in the photograph of Fig. 3.7. The laser tubes are parallel and separated by a distance of 1 inch. They utilize a common flat mirror, 1½ inches in diameter; two, one meter radii of curvature mirrors in a common mirror mount at the other end complete the cavity.

The close mechanical coupling of the two laser cavities results in an effective increase in the thermal and acoustic stability of the system; that is, a vibration which affects the length of one cavity will to a first order affect the length of the other one equally. When the two lasers are heterodyned, the difference frequency will not contain the perturbations introduced by vibrations. The same reasoning also applies to the slower variations in output frequency resulting from thermal causes. It has been determined that this cavity configuration reduces the effect of such disturbances by a factor of about 3000 [22].

In order to increase the overall mechanical stability of the mirror mounts, they were designed to be massive (about 20 pounds apiece) with no provision for angular adjustment of the individual mirrors. Instead, precision machining of the mounts was relied upon to assure approximate mirror alignment. To make any final adjust-

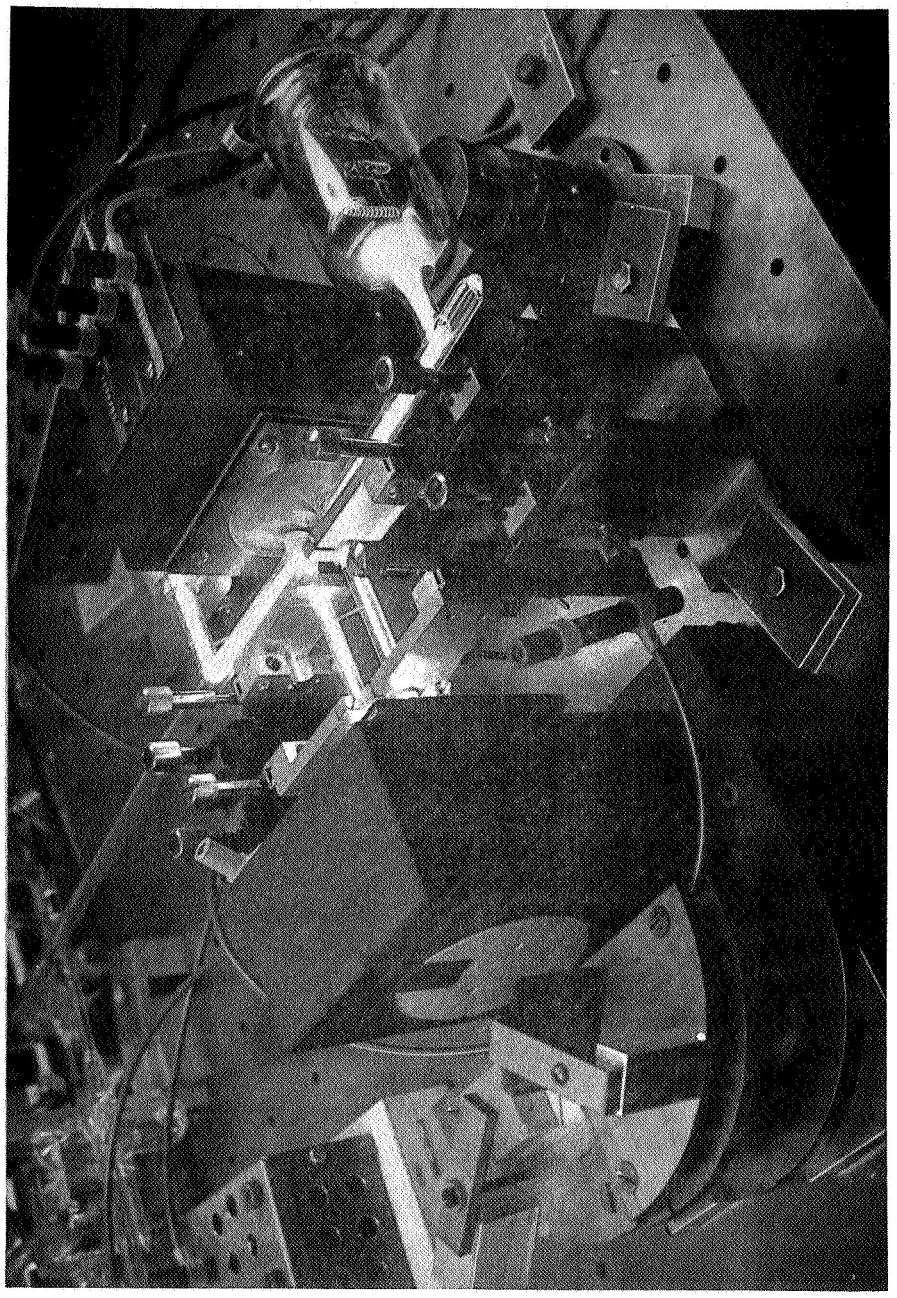

Fig. 3.7. Photograph of dual laser cavity.

ments, a mirror mount was rotated and one end elevated with brass shim stock.

The discharge tubes, individually mounted on modified micrometer microscope slide adjusters, can be aligned in the cavity using conventional techniques [23]. In order to operate both lasers simultaneously, the test laser tube is aligned first (since its position is fixed by attachment to the vacuum system) by adjusting the mirrors. The reference laser is then aligned by positioning the tube in the cavity. It is first placed in an approximately correct location and aligned with the flat mirror; the tube is then moved strictly perpendicular to its axis until alignment with the curved mirror is obtained. If any difficulties are experienced at this point, a mirror mount may be rocked slightly around the position at which the test laser operates to reveal the precise location of signal laser operation. Once the beam is found, it is a simple matter to obtain simultaneous oscillation in both cavities.

The overall stability of the system as described above is perhaps best illustrated by noting that under typical operating conditions on a normal workday the beat frequency was found to drift over a frequency range of $\pm$ 1 MHz. in a period of two minutes; during this time the frequency of each laser shifted by about 20 MHz.

3.7 Detecting and Measuring the Beat Frequency

Following the analysis of Oliver [24], the mechanics of

the detection process will be briefly outlined. The component of the electric field at the surface of the photodetector due to the signal laser is equivalent to

$$e_s(t) = E_s \sin \omega_s t$$

similarly, the field due to the local oscillator has the form

$$e_o(t) = E_o \sin (\omega_o t + \phi)$$

where ϕ is an arbitrary phase angle included for completeness. The output from the detector is proportional to the square of the resultant electric field or

$$i_s = \gamma [e_s(t) + e_o(t)]^2 = \frac{\gamma}{2} \Big[E_o^2 (1 - \cos 2\omega_o t) + E_o E_s (\cos [(\omega_s - \omega_o) t - \phi] - \cos [(\omega_s + \omega_o) t + \phi]) + E_s^2 (1 - \cos [2\omega_s t + \phi]) \Big]$$

Here γ relates the free space field strength to the current emitted from the photo-sensitive detector and is given by

$$\gamma = \frac{A e \eta}{2Zh\nu}$$

where A is the detector area, h is Planck's constant, η the quantum efficiency of the detector and Z is the impedance of free space. Since the detector does not respond to optical frequencies, the

components of the output current due to ω_s and ω_o average to zero leaving

$$i_s = \frac{\gamma}{2} (E_o^2 + E_s^2) + \frac{\gamma}{2} E_o E_s \cos [(\omega_o - \omega_s) t - \phi]$$

The a.c. component of this contributes to the signal output; the d.c. component results in the generation of shot noise within the detector with the resultant r.m.s. noise current given by

$$\overline{i_n^2} = 2 e B \bar{i} = e B \gamma (E_o^2 + E_s^2)$$

considering only the shot noise, the signal to noise ratio, S/N, of this system with bandwidth B is given by

$$S/N = \frac{\overline{i_s^2}}{\overline{i_n^2}} = \frac{\gamma}{eB} \frac{E_o^2 E_s^2}{E_o^2 + E_s^2} = \frac{An}{2Zh\nu B} \frac{E_o^2 E_s^2}{E_o^2 + E_s^2}$$

Physically, the signal and local oscillator beams are combined by the beam splitter-mirror combination as shown in Fig. 3.3. If the difference frequency is to be detectable, the relative phase difference between the wave fronts of the two beams must not vary appreciably over the surface of the detector. This has two implications: The individual beam wave fronts must not be appreciably distorted by interposed optics before they are combined at the beam splitter, and the angular separation θ_D between the component beams must satisfy the equation

$$\theta_D < \frac{\lambda}{2D}$$

For λ = 6328 Ang. and a spot size D/2 of ½ mm., $\theta_D \approx$ 2 minutes of arc. The alignment is accomplished in practice by simultaneously superimposing the two beams at the interface of the beam splitter and at some distant point. Attempts to improve the detector output by further adjustment indicated that the alignment performed in this manner is essentially optimum.

The operation of the lasers with the perturbation applied to the piezo-electric element can result in a considerable broadening in the width of the beat frequency. However, if a single oscillator is used to drive both crystals so that the amplitude and phase of the perturbation is identical on each laser, the resultant beat frequency linewidth is reduced. This is illustrated in Fig. 3.8. Oscillograph a shows the beat frequency with 100 mv. peak to peak perturbation applied only to one laser. Oscillograph b shows the beat frequency with the same perturbation applied to both lasers. The amplitude of that applied to the second laser has been "peaked" to attain a minimum dispersion. If the two lasers were not thus "phase locked", the width of the beat frequency would be double that shown in oscillograph a. This technique thus reduces the beat frequency width by about a factor of ten for this particular perturbation amplitude; correspondingly, the accuracy with which frequency measurements can be made improves by this same factor.

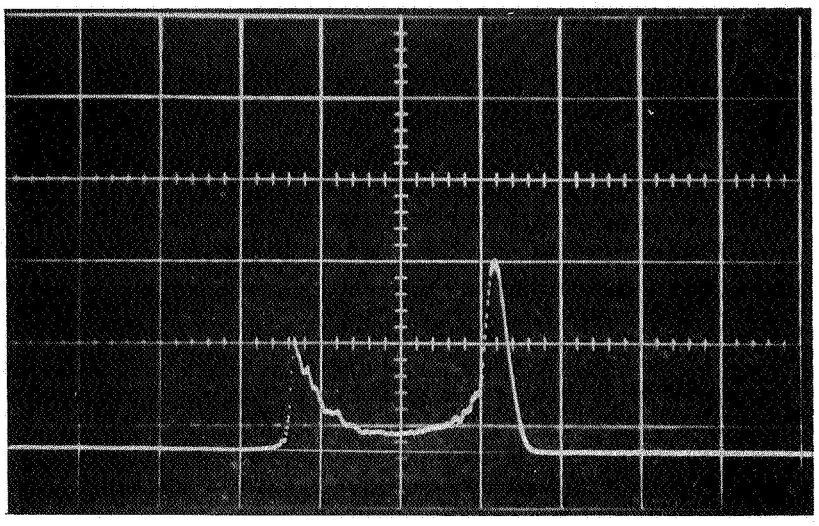

Fig. 3.8 a. Beat frequency between two lasers with perturbation applied to one laser. Sweep speed; 20 msec./cm. Dispersion: 150 kHz./cm.

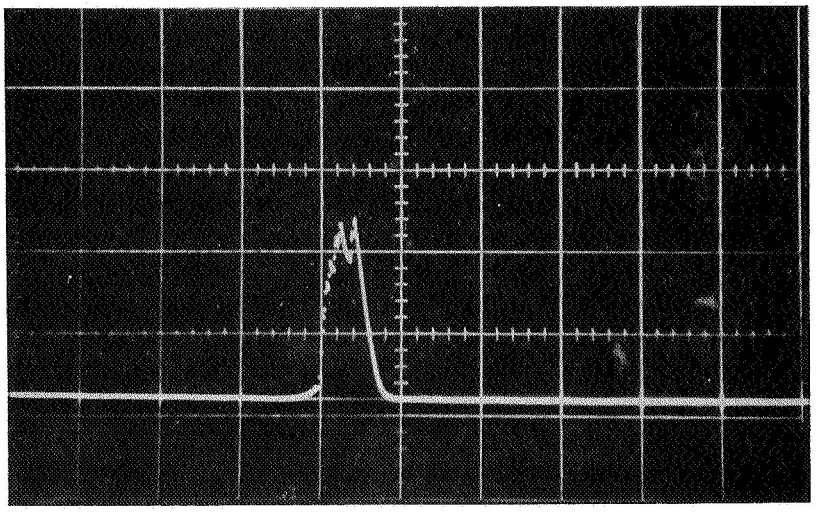

Fig. 3.8 b. Beat frequency with perturbation applied to both lasers. Sweep speed and dispersion same as above.

All frequency measurements were made using a Tektronix model 1L20 spectrum analyzer. The frequency calibration of this instrument was considered unreliable, however, so it was constantly referenced to a Hickok, model 292X, crystal controlled frequency generator. This instrument was previously calibrated against a Tektronix time mark generator and found to have an error of less than 3% of that read on the dial indicator over the frequency range 7 - 70 MHz. and an error of less than 5% for frequencies below this.

IV. EXPERIMENTAL RESULTS AND DISCUSSION

4.1 General Results

The peak frequency shifts of the 6328 Ang. neon line with changing discharge tube pressure for various combinations of helium and neon isotopes are shown in Figs. 4.1. They are representative of a large number of curves which were obtained.

General characteristics of the curves are: (1) they are monotonic, (2) the frequency increases with pressure (a blue shift), (3) the magnitude of the slope of the curve ($\Delta f/\Delta p$) varies from 17½ to 23 MHz/torr depending on the helium and neon isotopes contained in the discharge, and (4) as shown in Fig. 4.2, $\Delta f/\Delta p$ is independent of the helium-neon pressure ratio within the limits of error of the experiment. Some other features associated with the laser peak frequency which were found are: (5) increasing the helium partial pressure (total pressure constant) increases the frequency, (6) no measurable shifts were found with discharge tube current or (7) intensity of the laser beam, and (8) the peak frequency was a very sensitive function of the laser tube position in the cavity with the maximum frequency shift obtained by repositioning a 1 mm. bore discharge tube being 25 MHz.

Also, in the course of this study the frequency difference between the 6328 Ang. lines of the Ne^{20} and Ne^{22} isotopes was measured and found to be 930 MHz. with an estimated error of

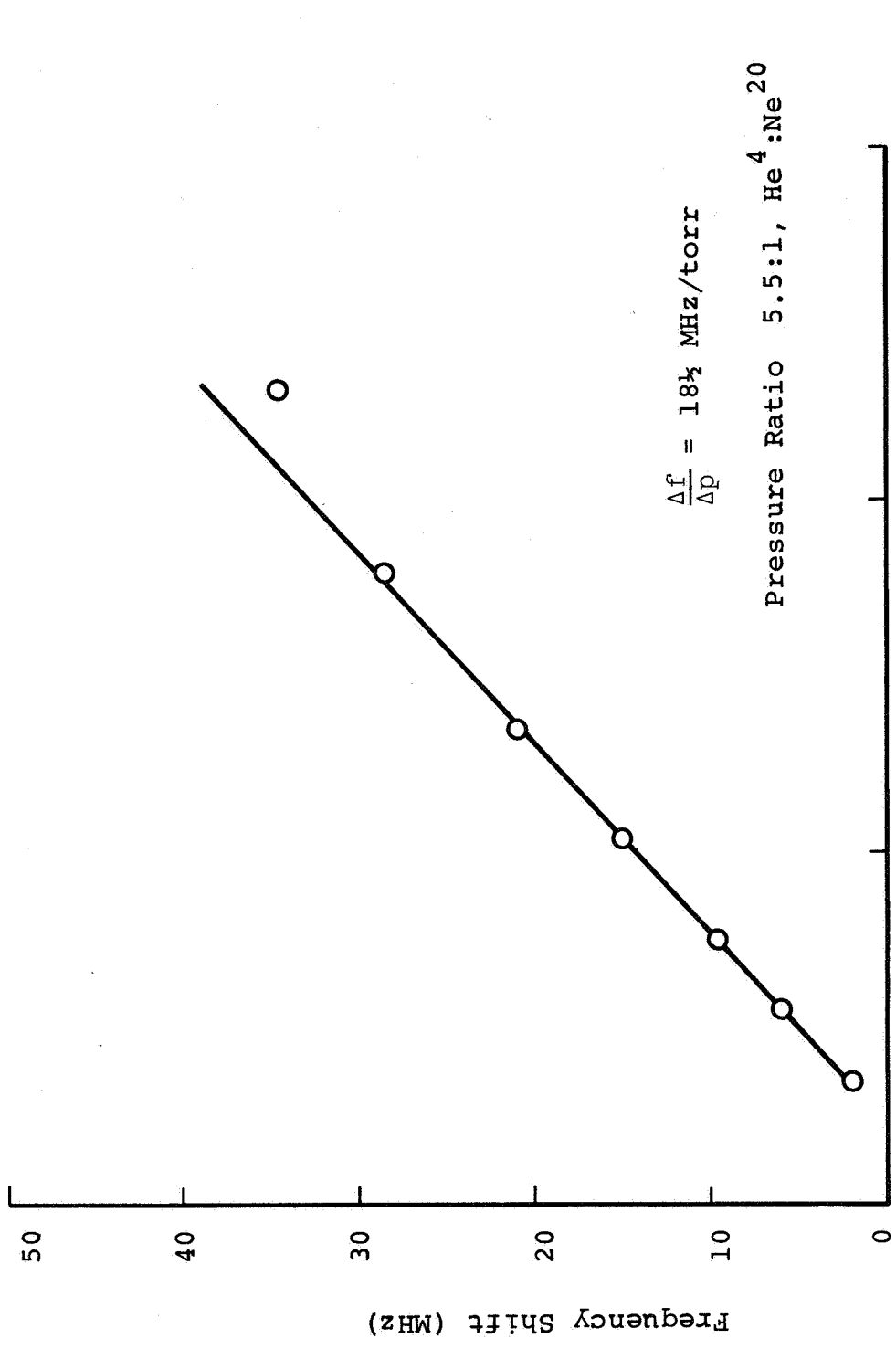

Fig. 4.1 a. Center frequency shift with pressure of the 6328 Ang. transition in Ne.

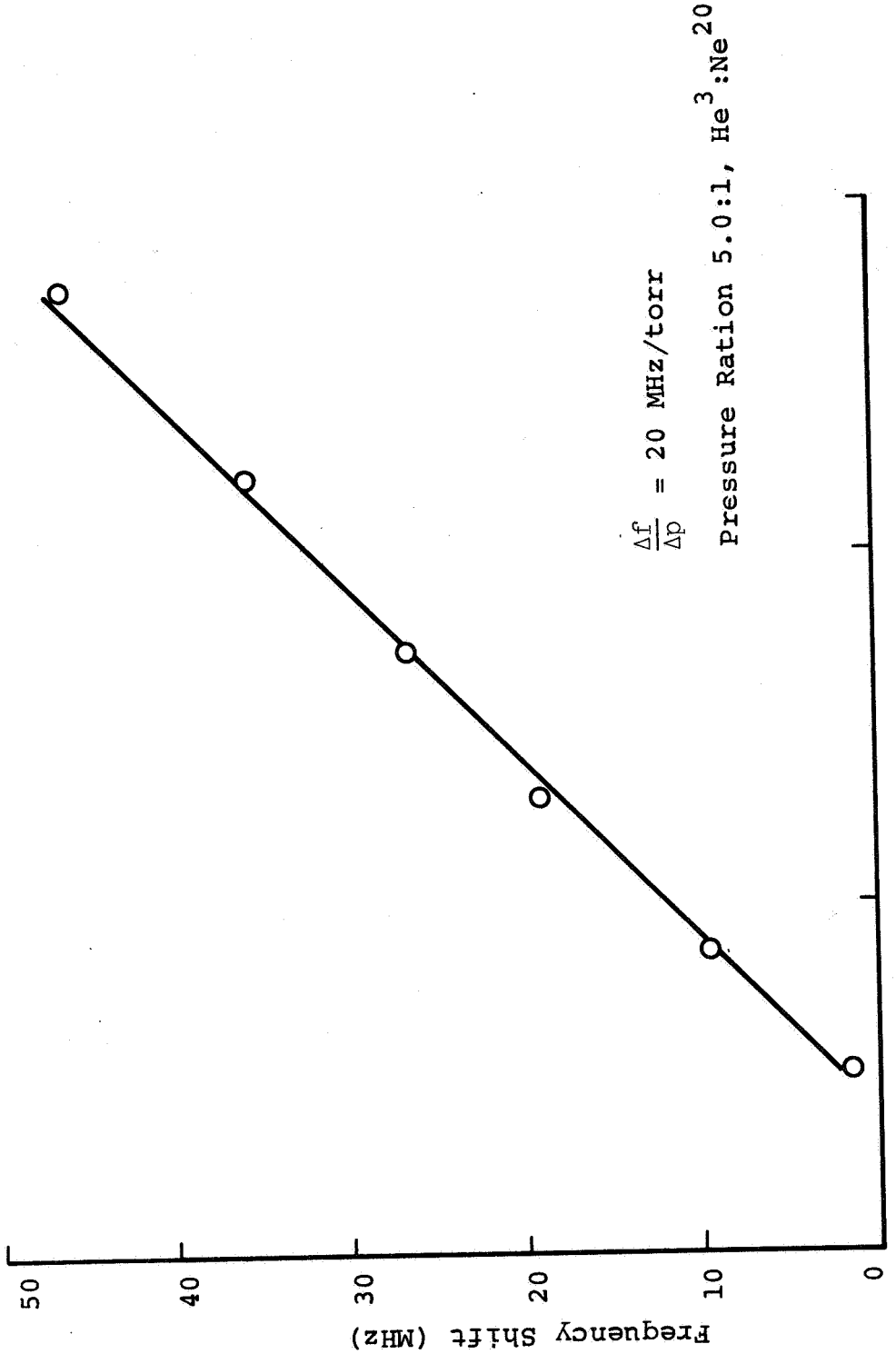

Fig. 4.1 b. Center frequency shift with pressure of the 6328 Ang. transition in Ne.

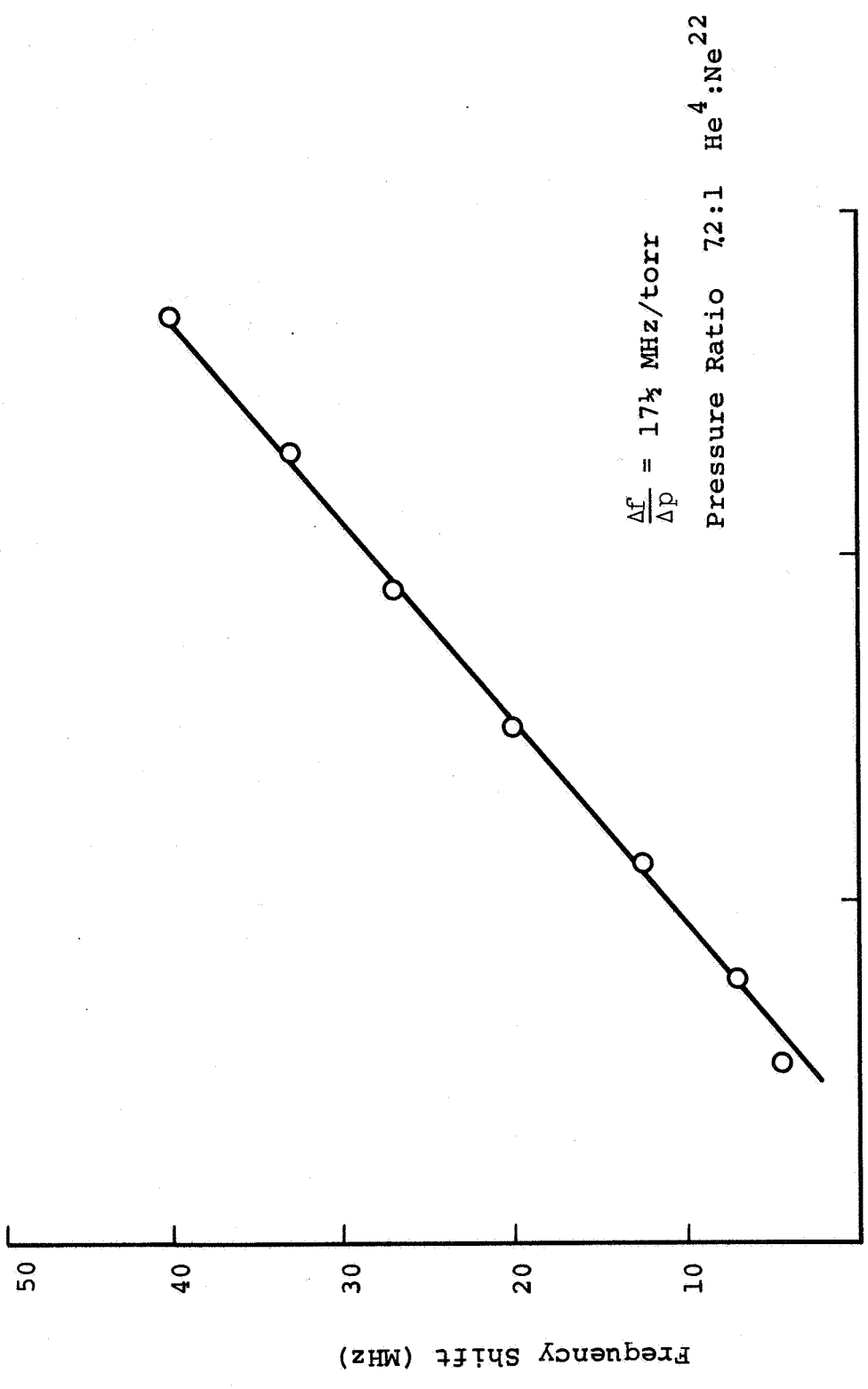

Fig. 4.1 c. Center frequency shift with pressure of the 6328 Ang. transition in Ne.

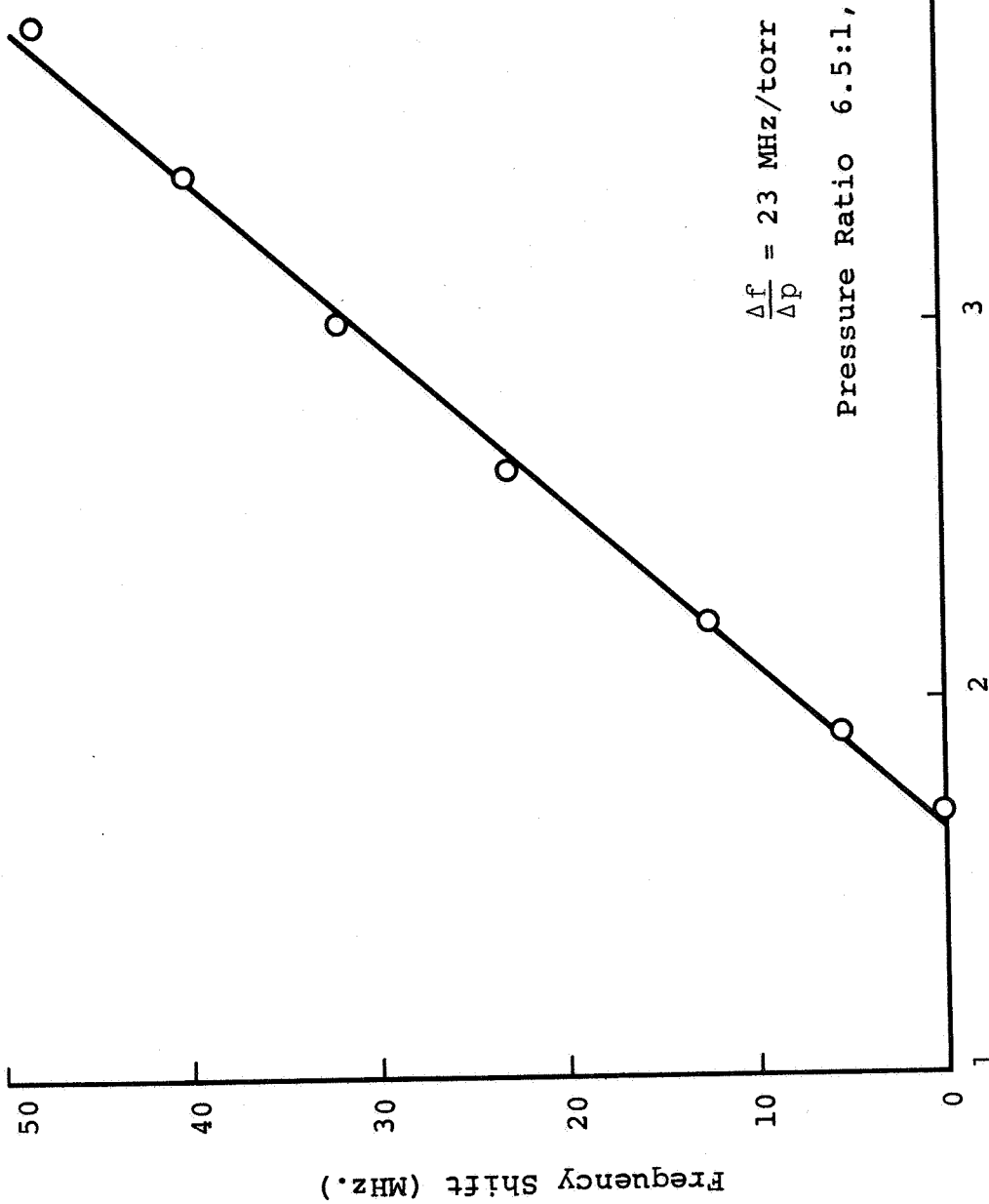

Fig.4.1 d. Center frequency shift with pressure of the 6328 Ang. transition in Ne.

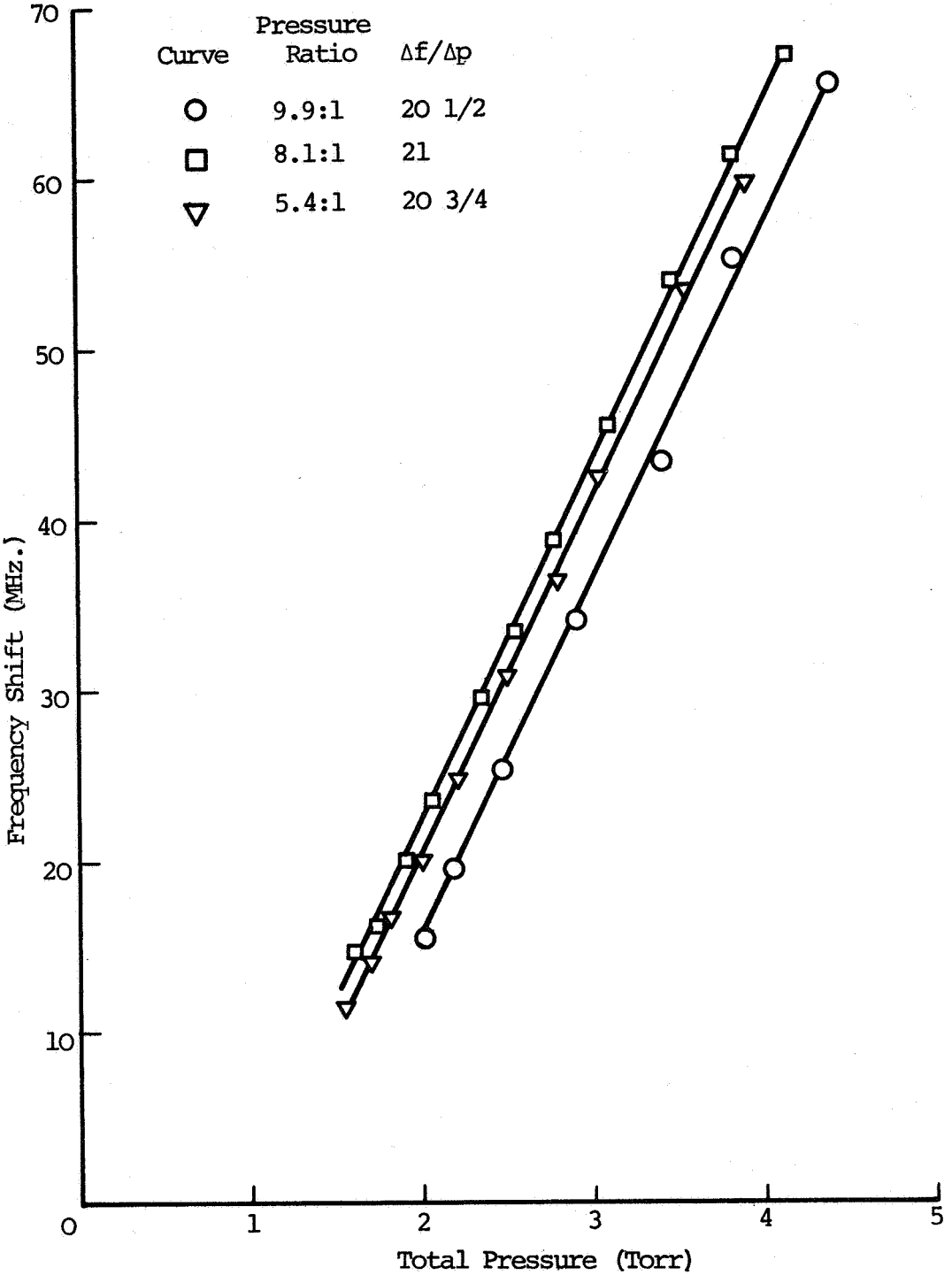

Fig. 4.2 Center frequency shift with pressure of the 6329 Ang. line in neon for various He^3-Ne^{20} pressure ratios.

± 70 MHz. This compares favorably with the value of 989 MHz. previously reported [25].

4.2 Specific details

The frequencies noted on the vertical axes of the graphs of Figs. 4.1 do not represent the absolute frequency difference between the two lasers; they are completely arbitrary with the zero frequency being chosen strictly for convenience. In the same regard, no frequency correspondence is meant to be implied between the curves of the various graphs. Each point on the pressure-frequency curves represents an average of five readings; normally they fell within a range of ± 1 MHz.* The points were obtained using a test laser with a tube of 1 mm. bore and a reference laser with a 1½ mm. bore; each had an active discharge length of 8 cm. and a nominal power output of one milliwatt. The cavity length was 15 cm. and each laser was operated in the lowest order transverse mode. The tubes were shielded from stray magnetic fields by mu-metal with the insertion of the shielding causing a frequency shift of less than 1 MHz.

The frequency difference between the 6328 Ang. lines of the two isotopes of neon exceeded the response of the RCA 6655A

---

*This indicates that each laser can be reset to within ±½ MHz.

photomultiplier tube (500 MHz.) used to detect the beat frequency between the two lasers, this necessitated the use of a reference tube filled with the neon isotope corresponding to that in the test laser. Both reference lasers were identical except for the neon isotope content. They were filled to a pressure of 3.2 torr with He^3 and Ne in the ratio of 8.5 to 1.

Because of the cavity configuration and the 1½ mm. bore tube used for the reference laser, diffraction losses for the lower order transverse modes were about equal; consequently, the laser tended to oscillate in something other than the lowest order transverse mode. To induce oscillation in the desired mode, diffraction losses were increased by moving the tube off the optical axis of the cavity in order to use the tube wall as an aperture stop. The problem was not encountered with the test laser because, with a tube diameter of only 1 mm., diffraction losses were great enough to prevent oscillation in all but the desired mode [26].

The sign of the slope of the curves was obtained by determining the relative frequency position of the two lasers and relating this to the direction of the beat frequency change with pressure. The relative frequency position of a laser is easily determined if the polarity of the piezo-electric ceramic associated with it is known (the length of the ceramic may increase or decrease with an increase in voltage depending on polarity). Assuming an increase in ceramic length with voltage, the cavity length decreases

causing the laser frequency to increase. In order to ascertain that the ceramic length increased with voltage, the effect was compared with the alteration of the cavity length by the slight motion of a mirror mount. A further verification of the indicated interpretation of the slope was obtained when a measurement was made of the frequency difference between the 6328 Ang. lines of the two isotopes of neon*, the result being that the Ne^{22} isotope had the higher frequency as expected.

The effect of changing the partial pressure of helium in the gas was determined by adding additional helium to the laser after the last point had been recorded at the low pressure end of the curve. The new total pressure was measured and the beat frequency compared to that obtained previously at the same pressure. In every case the frequency increased slightly with the increased partial pressure of helium as compared to that obtained previously at the same total pressure. No precise measurements were able to be made although indications are that doubling the helium partial pressure increased the peak frequency of the laser by about 4 MHz. for identical total pressures. This value is what would be expected if the frequency shift were proportional only to the partial pressure

---

* In making this measurement, the frequencies of those parts of the intensity curves having a zero slope were obtained and the results added in an appropriate fashion. This allowed the determination of the isotopic frequency difference without exceeding the frequency response of the detector.

of helium. Originally, an attempt was made to obtain pressure-frequency curves for various He^3-Ne^{20} partial pressure ratios ranging from 5:1 to 11:1; however, the peak frequency of the reference laser changed sufficiently from one test to another (because of random motions of the laser tube) to completely mask the sought-after differences. In fact, curves representing the same partial pressure ratio could not be reproduced except for the slope. They always showed a random shift parallel to the frequency axis. Fig. 4.2 shows a series of three curves for various pressure ratios of He^3-Ne^{20} taken several hours apart. The data points on the graph represent the heterodyne frequencies actually measured; the zero frequency position was not shifted here as it was for Figs. 4.1. The curves are indicative of the random shift in frequency with partial pressure ratios which were found. They are of further interest, however, in that they show the slope $\Delta f/\Delta p$ is insensitive to the partial pressure of the gases within the limits of error of the experiment. More will be said on this later.

The effects of residual impurities in the gases* and unavoidable contaminants from the vacuum system were measured by noting the frequency before and after the vaporization of a barium getter in the tube after it was filled with a new charge of gas; no

---

* The He^3, Ne^{20} and Ne^{22} were purchased from the Monsanto Research Corp., Miamisburg, Ohio; the He^4, from the Linde Co., Tonawanda, New York.

discernible difference in frequency was found.

The laser peak frequency was found to be a sensitive function of the distance between the optical axis of the cavity and the axis of the discharge tube. An effort was made to measure the shift in frequency per unit distance of movement of the 1 mm. bore laser tube transverse to its axis, but because of the close alignment tolerances on the system the tube could only be moved a maximum of 0.2 mm. A sufficient amount of information was gained to allow some rather qualitative conclusions, however. Initially the axes of the tube and cavity were rendered approximately coincident by peaking the output power; as the axes were separated, the peak frequency of the laser was found to increase. Movement of the tube 0.1 mm. off center increased the frequency in excess of 20 MHz. Further movement of the tube failed to produce reliable data because of difficulties in maintaining the Lamb dip. A 3 mm. bore tube with a 10 cm. active discharge length was constructed in order to obtain more quantitative results on the frequency shift with tube position. With this tube it was found necessary to place a 1½ mm. diameter aperture stop adjacent to the spherical mirror to prevent transverse modes other than the lowest order one from oscillating. Because of the diffraction losses induced by the stop, the tube could be moved a maximum of 0.4 mm. off axis before laser action ceased. It may be noted parenthetically that the laser intensity was very weak because of the large bore and short length. Data was taken using He^3 and Ne^{20} in a 10:1 mixture with total pressure of 1½ torr and also in an

8:1 mixture with a 2 torr total pressure. Measurement of the frequency shift along the diameter of this tube yielded a null result within the limits of accuracy of the data obtained. The conclusions which may be drawn from this limited amount of data are that the peak frequency shift due to discharge tube movement is small near the center of larger bore tubes. In smaller diameter tubes, the effect is quite significant.

In the course of making the above tests on the 3 mm. bore tube, it was observed that the laser beam intensity was also a function of radius and varied by at least a factor of two. Since the peak frequency did not vary with position in this case, the conclusion is partially substantiated that it is independent of laser power. A further fact supporting this position is that the beam intensity varied with discharge tube current yet no frequency shift was observed. Admittedly, two parameters were changed simultaneously (beam intensity and electron density) but it is highly unlikely that each would exactly counteract the other to produce the observed null result.

A final phenomena which was noted in the course of this study is that the magnitude of the slope $\Delta f/\Delta p$ was also dependent on the bore diameter of the discharge tube. The slope measured in He^3-Ne^{20} in the 1 mm. tube was about 20 MHz./torr. Less extensive data in a tube of 1½ mm. diameter indicated a shift of about 18 MHz./torr.

4.3 Factors Affecting the Peak Frequency of the Atomic Transition

The shift in frequency of spectral lines in discharge tubes is a much studied phenomena (see for instance references 27 and 28). All of the existing theories are, however, very complex and, at best, are able to provide only qualitative agreement with experiment. This is due primarily to difficulties in developing an understanding of the atomic interaction forces for the excited states involved. In essence the theories assert that collisions (in particular small angle or "soft" collisions) are chiefly responsible for the observed shifts, and that the magnitude of the shift is proportional to collision frequency.

Assuming that collisions are responsible for the observed shift in frequency of the 6328 Ang. neon line in a laser tube, several likely collision processes with the neon excited state are immediately evident as possible explanations. They are:

(1) $Ne^* + e \rightarrow Ne^* + e + \Delta E$

(2) $Ne^* + Ne \rightarrow Ne^* + Ne + \Delta E$

(3) $Ne^* + He^* (2^1S) \rightarrow Ne^* + He^* (2^1S) + \Delta E$

(4) $Ne^* + He^* (2^3S) \rightarrow Ne^* + He^* (2^3S) + \Delta E$

(5) $Ne^* + He \rightarrow Ne^* + He + \Delta E$

where Ne^* represents neon in the excited $3s_2$[†] state, e an electron,

---

† Paschen notation.

Ne a ground state neon atom, He^* (2^1S) a metastable helium atom in the 2^1S state, He^* (2^3S) a metastable helium atom in the 2^3S state, He a ground state helium atom, and ΔE the change in energy of the excited neon atom which takes place as a result of the encounter. The populations of any other excited states are presumably not great enough to seriously perturb the lasing transition and may be neglected.

With regard to process (1), it is known that the average electron density is proportional to discharge current [29] and the average electron temperature is largely independent of current [30] in the region of interest here. Because the collision frequency is proportional to density and temperature, an increase in discharge tube current should be accompanied by a shift in the peak frequency of the laser. Since no such shift is found, this mechanism may be discounted. Concerning collisions with the ground state atoms, the red shift with increasing pressure of the 6328 Ang. line in a pure neon discharge is attributed to this mechanism [31]. It seems likely that this same red shift would be observed, despite the presence of helium in the discharge, if this were the dominant shifting mechanism. Since a blue shift is observed, this process, too, may be discounted. Processes (3) and (4) may be treated together as will become apparent. Both metastable helium levels are excited primarily by collisions with electrons and to a much less extent by cascade from upper lying excited states. White and Gordon [32] have experimentally verified the current dependence of

the 2^1S metastable population in a helium-neon discharge tube. Since the excitation mechanisms for both metastable levels are essentially similar, it seems reasonable to ascribe this type of dependence to the 2^3S level as well. Hence, if either process (3) or (4) is responsible for the shift, the peak frequency should be sensitive to current. Again, this is not found to be the case. Concerning process (5), collisions between the excited neon atom and ground state helium atoms, there is some evidence which suggests that this mechanism is responsible for the observed frequency shifts. Namely, that increasing the helium partial pressure in the laser tube increases the laser peak frequency. A similar increase in peak frequency with the addition of helium has been found in the spectra of alkali atoms by others [28, 33]; it is attributed to repulsive forces between the two interacting bodies. A further observation is necessary on this mechanism, however. Lindholm's theory of spectral line widths and shifts [27] predicts that, for low pressures, the frequency shift, f, should be proportional to the partial pressure of the perturbing gas and related to the average relative velocity $< v >$ between the perturbing and perturbed particles; that is

$$f \propto p_{He} < v >^{3/5}$$

Letting κ represent the helium-neon pressure ratio, it is easily shown that

$$\frac{\Delta f}{\Delta p} = \frac{\kappa}{\kappa + 1} < v >^{3/5} \qquad (4.1)$$

where Δp represents the change in total pressure. Allowing $S = \Delta f/\Delta p$ for convenience, the ratio of slopes for the two pressure ratios, κ_1 and κ_2, is found to be

$$\frac{S_1}{S_2} = \frac{\kappa_1 (\kappa_2 + 1)}{\kappa_2 (\kappa_1 + 1)}$$

Here, the ratio of velocities has been set equal to one because the change in relative velocity between colliding particles due to a change in pressure ratio is negligible. This relation shows an increase in slope of about 10% upon alteration of the gas ratio from 5:1 to 10:1, or a slope change from 20 MHz./torr to 22 MHz./torr for the He^3-Ne^{20} mixture. Reference to Fig. 4.2 shows that such a change has not been found although the accuracy of the experiment was marginal for its detection. In conclusion, it is at least consistent with the above related facts to ascribe the observed blue shift to collisions between the excited neon and ground state helium atoms.

It is possible to make some observations on the velocity dependence of equation 4.1 by considering gas mixtures having the same partial pressure ratios but using different isotopes of helium. Again taking the ratio of slopes, it is no longer possible to set the ratio of relative velocities equal to one. It may , however, be

simply determined with less than 5% error by treating the neon atoms as particles with zero velocity. With the assumption that the gas temperature in mixtures containing different isotopes of helium is approximately the same, the ratio of velocities is found from the conservation of energy principle to be $v_1/v_2 = (m_2/m_1)^{\frac{1}{2}}$; here, v_i is the velocity of a particle with mass m_i. Thus, the ratio of slopes for the same pressure ratio but different helium isotopes is approximately given by

$$\frac{S_1}{S_2} \simeq \left(\frac{m_2}{m_1}\right)^{3/10} \simeq \left(\frac{4}{3}\right)^{3/10} \simeq 1.1$$

Comparing this value with that measured, it is found that for mixtures containing Ne^{20} the ratio of slopes is 1.1 while for mixtures containing Ne^{22} the ratio of slopes is 1.3.

In the course of this investigation, it was thought that perhaps the collision probability between the interacting particles was influencing the slopes of the curves for the various isotopic mixtures. This may be seen be recognizing that the frequency shift is proportional to a probability of collision. Since the collision is of a resonant type, the probability is in turn related to the difference in energy between the helium 2^1S and the neon $3s_2$ levels - a difference which changes with the various combinations of isotopes. Calculations using the known differences in energy between the various isotopes show, however, a change in slope which is very much less than the observed value. The relatively strong dependence of the curve slope probably prevents the observation

of any effect of the probability.

A major weakness of the collision theories is that they fail to account for the dependence of the peak frequency on the discharge tube position in the cavity. In an effort to explain this, as well as other observed phenomena, Mayer [34] has proposed that the electric fields generated by ambipolar diffusion are responsible for the frequency shifts through the mechanism of the Stark effect. Using simple charged particle diffusion theory in the positive column of the gas discharge coupled with the second order Stark effect, he arrives at a value for the frequency shift from line center given by

$$f = -2.8 \times 10^{6} \, (Te/R)^{2} \, \eta \qquad (4.2)$$

where

$$\eta = \left[\frac{J_1 \, (2.405 \, r/R)}{J_o \, (2.405 \, r/R)} \right]^2$$

T_e is the electron temperature in units of 10 e.v., R the radius of the discharge tube in mm., and r is the distance from the tube axis. J_o and J_1 are the zero and first order Bessel functions. Without performing any numerical calculations, the utility of the above theory may be determined by inserting into equation 4.2 what is known of the electron temperature variations in the helium-neon laser discharge and comparing the predicted and observed frequency shift. As noted previously, the electron temperature is independent

of the electron density, no frequency change is predicted with discharge current in conformity with what is observed. An increase in gas pressure decreases T_e [30] resulting in an increase in frequency as is measured. However, it is known that the electron temperature increases with increasing helium partial pressure [35] and this would cause the frequency to decrease which is contrary to what is observed. A further inconsistency lies in the predicted frequency shift with position of the laser tube in the cavity. Fig. 4.3 shows the functional dependence of η on r and indicates that a decrease in frequency would be observed as the beam approaches the tube wall whereas an increase in frequency is actually measured. A few other interesting properties of equation 4.2 should be mentioned. A gas discharge containing He^3 has a higher electron temperature than an equivalent discharge containing He^4 [36]; consequently, the pressure-frequency curve of the discharge containing the former isotope will have the greater slope again in conformity with what is observed. Finally we may note that f has an inverse dependence on the radius of the discharge tube. The electron temperature is also dependent on the tube radius; fortunately, it decreases with increasing radius so that we are able to make the qualitative observation that the slope of the pressure-frequency curve will decrease with increasing tube diameter. Neglecting the effect of the tube radius on the electron temperature, the ratio of slopes S_1/S_2 for two tubes of radii R_1 and R_2 is found from equation 4.2 to be

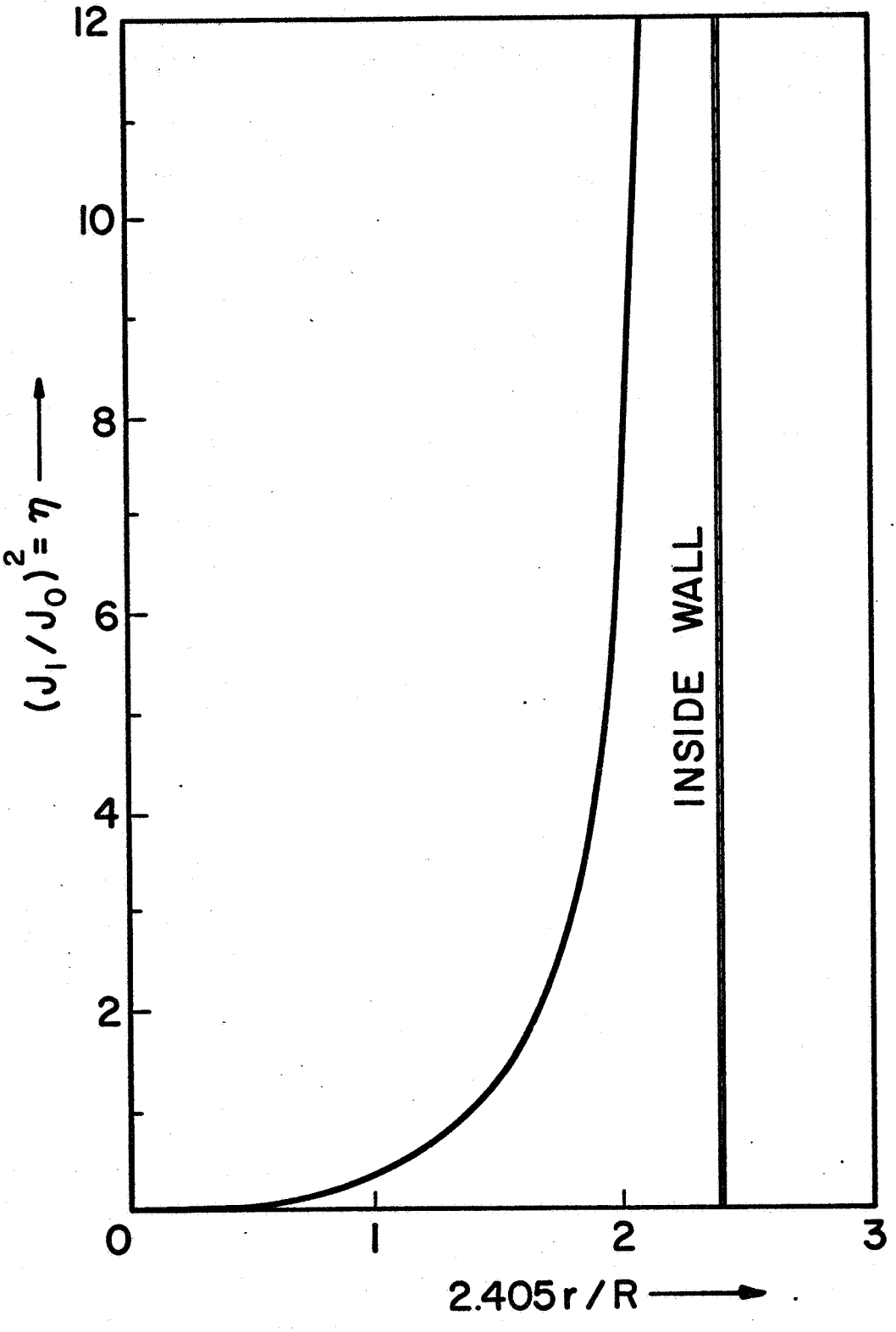

Fig. 4.3 The functional dependence of η on r .

$$S_1/S_2 = (R_2/R_1)^2$$

Using a slope of 20 Mhz./torr for S_1 with a tube radius of R_1 = ½ mm., a radius R_2 of .75 mm. gives a value for S_2 of 9 MHz./torr which is less than the measured value by a factor of two. Consideration of the electron temperature will lower this value of S_2 still further. In conclusion, though the theory offers some interesting insights into the possible mechanisms controlling the frequency of the laser, the inconsistencies between it and experimental observations are sufficient to warrant further study of the problem. It is well to remember, however, that it is presently the only theory which predicts a frequency variation with radial position or tube radius.

4.4 Comparison with other work

The results obtained for the frequency shifts with pressure in this work are not in agreement with those obtained by Bloom and Wright [37]. In the pressure range between 3 and 4 torr, they measured a red shift of approximately -20 MHz./torr. At lower pressures of 2 to 2.5 torr, the shift reaches a maximum and then reverses direction. It may be noted that they determined the sign of the slope, not by independently compressing the laser cavity but by observing the effects of the movement of the piezo-electric ceramic which may either expand or contract with the application of a voltage. (The slope cannot be determined until the ceramic polarity is known). The magnitude of the frequency shift above 3

torr approximates that obtained here, the work having been done in the same diameter tube (1 mm.). The apparent random frequency shift with increasing helium partial pressure obtained by them may be adequately explained by the discharge tube shifting its position slightly in the cavity (≈ .05 mm.) between successive curves.

The blue shift obtained here is in conformity with the results obtained by White [31]; however he measures a frequency shift in a He^3-Ne^{20} gas mixture of about 18 MHz/torr in contrast to the 20 MHz/torr obtained here. A possible explanation for this is that a laser tube with a bore diameter different from 1 mm. may have been used (the tube diameter was not specified in the report). As indicated previously, larger discharge tube diameters produce smaller slopes.

CHAPTER V

CONCLUSIONS AND RECOMMENDATIONS FOR FURTHER STUDY

In summary, the center frequency of the 6328 Ang. helium-neon laser is found to be significantly affected by gas pressure and (for small bore tubes) the position of the laser tube in the cavity. It is affected to a lesser extent by the helium-neon pressure ratios and isotopes of gas contained in the discharge. A further influencing factor is the discharge tube bore size, the increase of which appears to decrease the slope of the pressure-frequency curve. Frequency shifts ranging from 17 1/2 to 23 MHz per torr, depending on the isotopic content, were found in 1 mm. bore discharge tubes; they are summarized in Table I. The slopes of the curves were independent of the partial pressure ratios of the constituent gases. The frequency shift produced by lateral motion of the laser tube was found to be about 20 MHz per 0.1 mm. for a 1 mm. bore tube and negligible over a distance of $\pm$ 0.4 mm. from the center of a 3 mm. bore tube. The peak frequency was essentially independent of current. In addition, the frequency difference between the 6328 Ang. lines for the Ne^{20} and Ne^{22} isotopes has been remeasured and found to be 930 $\pm$ 70 MHz. in conformity with that already reported.

	He^3	He^4
Ne^{20}	20	18 1/2
Ne^{22}	23	17 1/2

Table I. The slopes of the pressure-frequency curves in MHz./torr for various combinations of He and Ne isotopes.

In consideration of this information, a laser serving as a frequency reference should utilize a discharge tube with a large bore. In view of the pressure shifts, a precise laser frequency may be difficult to maintain because of the effect of "gas clean-up" on the pressure and composition of the gas in the discharge tube [38]. These can be minimized, however, by using He^4 and Ne^{22} isotopes in the discharge (this combination of gases has the smallest value of $\Delta f/\Delta p$) and increasing the volume of the gas by means of an auxiliary chamber attached to the tube. These alternatives are adverse to high power output from the laser (gain decreases with increasing tube diameter and the use of He^3 in the discharge increases power by 25%) so that they must be weighed against the ultimate needs of the device. Finally, a simple calculation shows that in order to maintain a frequency stability of 10^{10} which is consistent with the capabilities of the electronic frequency control system, the discharge tube pressure must be maintained within a tolerance of less than .003 torr and the discharge tube position (for the commonly used 1 mm. tube) must be

maintained to within 0.25 microns.

Mechanisms possibly responsible for the observed frequency shifts have been investigated. Collisions between the excited neon atom and ground state helium atoms appear to be the most likely cause of the frequency shift with pressure. Collision phenomena is in no way able to explain the observed frequency shifts as a function of radius in a discharge tube, however. It has also been shown how electric fields caused by ambipolar diffusion may cause frequency shifts through the mechanism of the Stark effect. Here again, some basic inconsistencies exist between the predicted and observed phenomena. The conclusion of this phase of the study is that present theory is not well enough developed to predict the observed phenomena.

Several phenomena revealed in the course of this work are in need of further investigation. The center frequency of the 6328 Ang. transition has been found to be a function of radial position in the discharge tube; this should be studied further as a function of both gas pressure and discharge tube diameter with the hope of shedding some light on some of the basic mechanisms occurring in the discharge. To this end, also, further study is needed on the effect the discharge tube diameter has on the slope of the pressure-frequency curve.

APPENDIX A

DERIVATION OF A CONTROL SIGNAL FROM THE GAIN CURVE

One method of frequency stabilizing the helium-neon gas laser uses the bottom of the Lamb dip as a reference. An error signal is derived by perturbing the laser frequency, this produces an amplitude modulated beam which is then compared in phase with the perturbation.

The Lamb dip is essentially a Lorentzian hole in the peak of a Gaussian gain curve [39, 40]. The dip is primarily due to pressure effects and hence is much narrower than the Doppler broadened gain curve, thus the effect of the Gaussian may be neglected in this analysis. A Lorentzian curve has the form

$$I(x) = - C \frac{a}{x^2 + a^2}$$

where I is the intensity, a is related to the half width, c is some constant and $x = \nu - \nu_o$ where ν_o is the peak (or dip) frequency (this transformation is equivalent to making $x = 0$ the peak frequency). Suppose now a sinusoidal perturbation of amplitude x_1 and frequency ω is applied around some arbitrary point x_0, or

$$x = x_0 + x_1 \sin\omega t$$

The time dependence of the amplitude thus takes the form

$$\frac{dI}{dt} = \frac{dI}{dx}\frac{dx}{dt} = 2\,ca\,\frac{x}{(x^2 + a^2)^2}\,\omega x_1 \cos\omega t \qquad (2)$$

for small excursions about the peak frequency, $a >> x$ amd x may be neglected in the denominator.* Combining equations 1 and 2 gives

$$\frac{dI}{dt} = ca^{-3}\,(2x_o\,x_1 \cos\omega t + \omega x_1^2 \sin 2\omega t)$$

The second harmonic content may be filtered out of the signal so that we are left with the form,

$$\frac{dI}{dt} = kx_o \cos\omega t = k\,|x_o|\cos(\omega t + \phi)$$

where $k = 2cx_1\omega a^{-3}$. The above relationship emphasizes the equivalence of $\pm x_o$ to a value for ϕ of 0 or π respectively. Thus the distance from the peak is determined by the amplitude of the intensity modulation while the side of the Lorentzian at which the laser operates is determined by comparing the phase of the intensity modulation with that of the input signal. These provide all the necessary information for the control system.

---

* Under conditions suitable for frequency stabilized laser operation, the Lamb dip has a full width at half maximum of approximately 400 MHz. whereas the value of x_1 is of the order of 1 MHz. so that this is a valid approximation.

APPENDIX B

LASER FREQUENCY CONTROL UNIT

A block diagram of the laser frequency control unit is illustrated in Fig. 3.4. The 5 kHz. oscillator frequency modulates the laser by varying the length of a piezo-electric ceramic to which one of the laser mirrors is attached. The resulting amplitude modulated laser beam is detected by a Dumont 6467 photomultiplier. After amplification by the 60 db. gain, ½ kHz. bandwidth tuned amplifier, the signal is fed, along with an output from the oscillator, into the phase detector. The output of the detector, as monitored by the peak frequency indicator, reveals the location on the gain curve at which the laser operates. The laser frequency control is simply a source of well filtered variable d.c. voltage used to bias the piezo-electric crystal allowing adjustment of the cavity length. The complete circuitry is shown in Fig. B-1. For most efficient operation of the phase detector, the peaks and nulls of the two input signals should coincide. The coincidence is established by phase shifting the signal from the photomultiplier tube with the π type LC network between the two tuned amplifier stages. The circuitry is otherwise self-evident.

In actual operation, each laser is manually tuned to its center frequency by adjusting the length of the cavity until a zero output is obtained from the peak frequency indicator which is a 25-0-25 microameter. A study of the gain curve pictured in Fig. 3.2

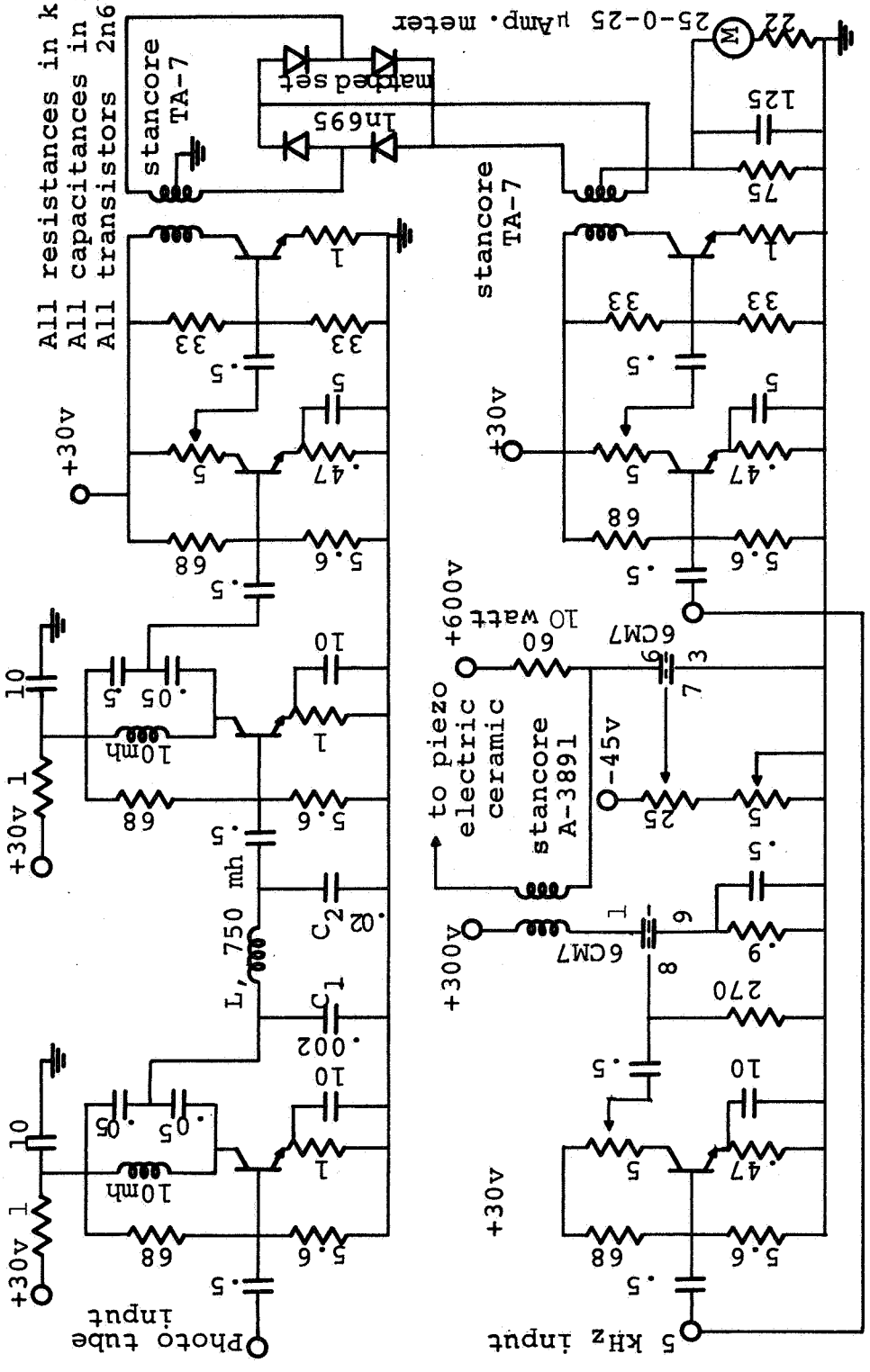

Fig. B-1 Laser frequency control unit

indicates that at least three null readings will be generated as the laser is tuned across the gain curve, one for each peak and one at the central dip, the central one being, of course, the desired null. Since the output of the phase detector can be made to correspond to the slope of the gain curve (positive output for positive slope) the proper null will be indicated by the ammeter needle passing through zero from left to right as the laser frequency is increased, the converse indicating a peak. The polarity of the phase detector may be tested by decreasing the gain of the laser until the Lamb dip disappears and then tuning across the gain curve, only a null corresponding to a peak will be detected and this may be correlated with the microameter movement.

APPENDIX C

DETERMINATION OF HE-NE PRESSURE RATIOS

The experiment necessitated the use of helium-neon gas mixtures with accurately known partial pressures. The particular design of the gas handling system and the use of the McLeod gauge to measure pressures required the use of a special technique to measure these. It is easily explained with the aid of the schematic diagram of Fig. C-1. The system is assumed evacuated and all valves closed. Valves B and C are opened and neon gas is admitted from the supply to the approximate pressure as noted by the Pirani gauge attached to the mixing chamber. Valves B and C are then closed and valve F open to evacuate the manifold section of the system. A pressure measurement is made with the McLeod gauge, then it too, is evacuated by opening valve A. With valve F closed, helium gas is bled into the mixing chamber until the approximate proper pressure is registered by the Pirani gauge. Now valve B is opened admitting the helium-neon gas mixture to the McLeod gauge where a measurement can be made. The gas pressure originally in the mixing chamber can then be computed if the ratio of the volumes the gas occupies before and after valve B is opened is known. This ratio has been computed with the aid of the expression

$$(V_1 + V_2)/V_2 = P_i/P_f = k$$

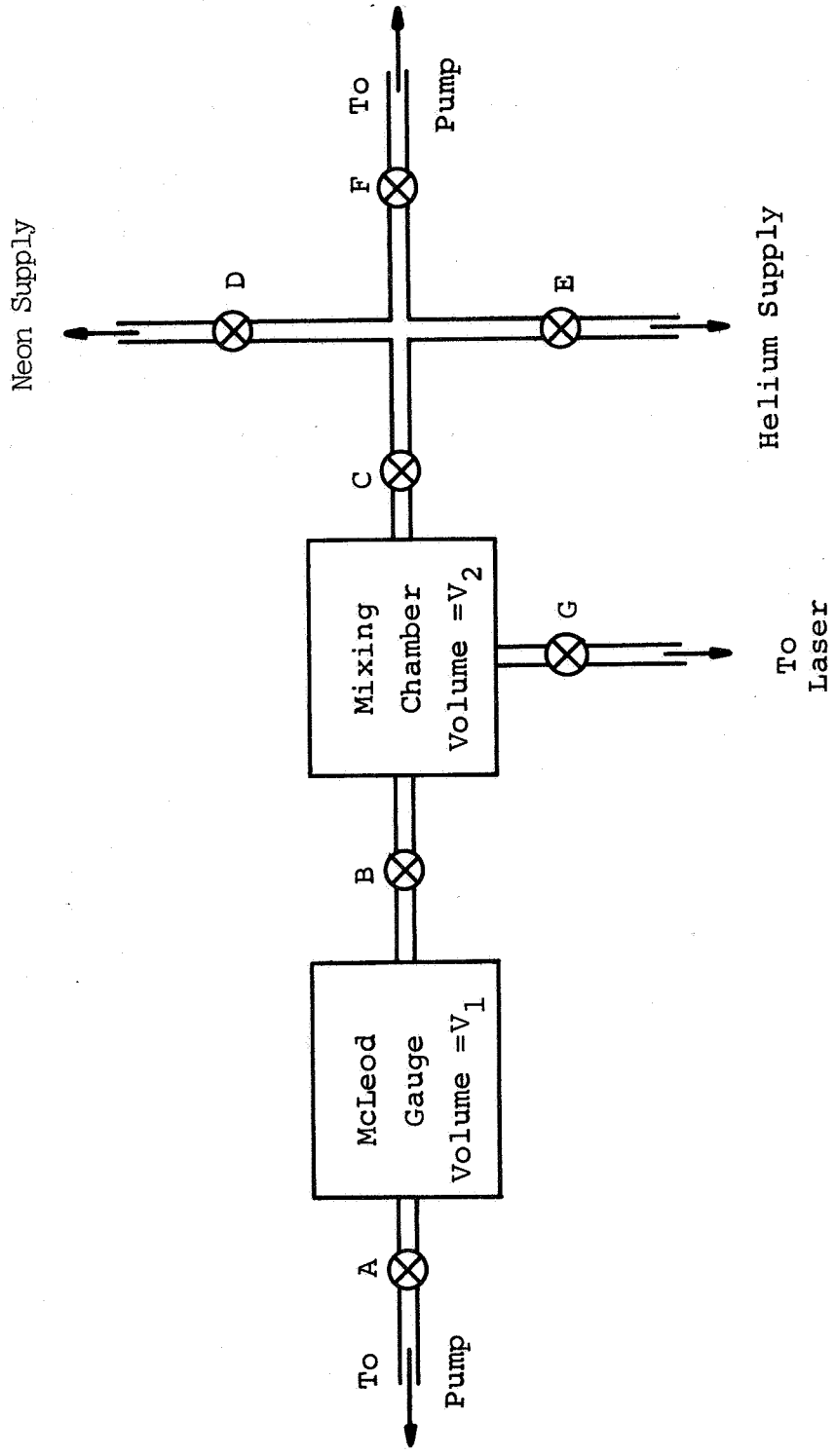

Fig. C-1 Diagram of gas handling system

where V_1 is the volume of the McLeod gauge, V_2 the volume of the mixing chamber, P_i the initial pressure in the mixing chamber, and P_f the final pressure in the McLeod gauge-mixing chamber combination. A series of ten measurements were taken of the pressure ratios and the results averaged to obtain a value for k of 1.76.

LIST OF REFERENCES

1. T. S. Jaseja, A. Javan, and C. H. Townes, "Frequency stability of He-Ne Masers and measurements of length," Phys. Rev. Letters, vol. 10, p. 165, March 1963.

2. B. L. Gyorffy and W. E. Lamb, Jr., "Pressure effects in the output of a gas laser," in Physics of Quantum Electronics. New York: McGraw-Hill, 1966 p. 602.

3. A. Szoke and A. Javan, "Effects of collisions on saturation behavior of the 1.15μ transition of Ne studied with He-Ne laser," Physical Review Vol. 145 p. 137, May 1966.

4. G. D. Boyd and H. Kogelnik, "Generalized confocal resonator theory," vol. 41, p. 1347, July 1962.

5. P. W. Smith, "Stabilized Single Frequency output from a long laser cavity," IEEE J. Quantum Electronics, vol. QE-1, p. 343, November 1965.

6. I. P. Kaminow, "Balanced optical discriminator," Appl. Optics, vol. 3, p. 507, April 1964.

7. S. E. Harris, "Demodulation of phase-modulated light using birefringent crystals," Proc. IEEE, vol. 52, pp. 823-831, July 1964.

8. E. A. Ballik, "Optical maser frequency stabilization and precise wavelength measurements," Phys. Letters, vol. 4, p. 173, April 1963.

9. A. D. White, "Frequency stabilization of gas lasers," IEEE J. Quantum Electronics, vol. QE-1, p. 349, November 1965.

10. W. R. C. Rowley and D. C. Wilson, "Wavelength stabilization of an optical maser," Nature, p. 745, November 1963.

11. K. Shimoda and A. Javan, "Stabilization of the He-Ne maser on the atomic line center." J. Appl. Phys. (pt. I) vol. 36, p. 713, March 1965.

12. W. R. Bennett, S. F. Jacobs, J. T. Latourette, and P. Rabinowitz, "Dispersion characteristics and frequency stabilization of a gas laser," Appl. Phys. Letters, vol. 5, p. 56. August 1964.

13. A. D. White, E. I. Gordon, and E. F. Labuda, "Frequency stabilization of single mode gas lasers," Appl. Phys. Letters, vol. 5, p. 97, September 1964.

14. I. Tobias, M. Skolnick, R. A. Wallace, and T. Polanyi, "Derivation of a frequency-sensitive signal from a gas laser in an axial magnetic field," Appl. Phys. Letters, vol. 6, p. 193, May 1965.

15. K. D. Mielenz, R. B. Stephens, K. E. Gillihand, and U. F. Nefflen, "Measurement of absolute wavelength stability of lasers," J. Opt. Soc. Am., vol. 56, p. 156, February 1966.

16. A. L. Schawlow and C. H. Townes, "Infrared and optical masers," Phys. Rev., vol. 112, p. 1940, December 1958.

17. P. Grivet and A. Blaquiere, Symposium on Optical Masers, J. Fox, Ed. Brooklyn, N.Y.: Polytechnic Press, pp. 69-93, 1963.

18. A. Javan, E. A. Ballik, and W. L. Bond, "Frequency characteristics of a continuous-wave He-Ne optical maser," J. Am. Opt. Soc., vol. 52, p. 96, January 1962.

19. W. E. Lamb, "Theory of an optical maser," Phys. Rev., vol. 134, p. A1429, June 1964.

20. A. Szöke and A. Javan, "Isotope shift and saturation behavior of the 1.15-μ transition of Ne," Phys. Rev. Letters, vol. 10, p. 521, June 1963.

21. S. F. Jacobs and P. J. Rabinowitz, "Optical heterodyning with a CW gas laser," in "Quantum Electronics III," P. Grivet and N. Bloombergen, Eds. New York: Columbia University Press, 1964, p. 481.

22. A. B. Larsen,"Electrons and metastable atom density measurements with a two wavelength laser heterodyne interferometer"(Ph.D Thesis Case Institute of Technology, 1966) p. 31.

23. T. P. Sosnowski, "Development of gas lasers for use in plasma diagnostics," (Masters Thesis, Case Institute of Technology, 1965) p.52.

24. B. M. Oliver, "Signal-to-noise ratio in photo electric mixing," Proc. IRE, vol. 49, p. 1960, December 1961.

25. R. H. Cordover, T. S. Jaseja, and A. Javan, "Isotope shift measurement for 6328 Ang. He-Ne laser transition," Appl. Phys. Letters, vol. 7, p. 322, December 1965.

26. Tingye Li, "Diffraction loss and selection of modes in maser resonators with circular mirrors," Bell System Tech. J., vol. 44, p. 917, May 1965.

27. The Shift and Shape of Spectral Lines, Robert G. Breene, Jr. New York: Pergamon Press, 1961.

28. S. Ch'en and M. Takeo, "Broadening and shift of spectral lines due to the presence of foreign gases," Rev. Mod. Phys., vol. 29, p.20, January 1957.

29. E. I. Gordon and A. D. White, "Similarity laws for the He-Ne gas maser," Appl. Phys. Letters, vol. 3, p. 197, 1963.

30. E. F. Labuda, and E. I. Gordon, "Microwave determination of average electron energy and density in He-Ne discharges," J. Appl. Phys., vol. 35, p. 1647, May 1964.

31. A. D. White, "Pressure and current dependent shifts in the center frequency of the Doppler-broadened ($2p_4 \rightarrow 3s_2$) 6328-Å Ne^{20} transition," Appl. Phys. Letters, vol. 10, p. 24, January 1967.

32. A. D. White and E. I. Gordon, "Excitation mechanisms of the He-Ne gas maser," Appl. Phys. Letters, vol. 3, p. 199, 1963.

33. Resonance Radiation and Excited Atoms, A. C. G. Mitchell, and M. W. Zemnsky, New York: Columbia University Press, 1961, p. 174.

34. F. J. Mayer, "Stark effect produced frequency shifts in the He-Ne laser," to be published.

35. R. T. Young, "Calculation of average electron energies in He-Ne discharges," J. Appl. Phys., vol. 36, p. 2324, July 1965.

36. A. D. White "Increased power output of the 6328-Å gas maser," Proc. IEEE, vol. 51, p. 11, November 1963.

37. A. L. Bloom and D. L. Wright, "Pressure shifts in a stabilized single wavelength helium-neon laser," Proc. IEEE, vol. 54, p. 1290, October, 1966.

38. R. Turner, K. M. Baird, M. J. Taylor, and C. J. Vander Hoeven, "Lifetime of helium-neon lasers," Rev. Sci. Instr., vol. 35, p. 996, August 1964.

39. W. R. Bennett, Jr., "Mode pulling in gas lasers," in Quantum Electronics III, P. Grivet and N. Bloombergen, Eds. New York: Columbia University Press, 1964, p. 441.

40. W. R. Bennett, Jr., "Hole burning effects in a He-Ne optical maser," Phys. Rev., vol. 126, p. 580, April 1962.